Theoret. chim. Acta (Berl.) 21, 335—367 (1971)

SCF-MO-LCGO Studies on Hydrogen Bonding. The Water Dimer

Geerd H. F. DIERCKSEN*
Max-Planck-Institut für Physik und Astrophysik, 8000 München 23, Germany

Received November 30, 1970

The hydrogen bond in the water dimer is studied within the SCF-MO-LCAO framework, using a large Gaussian basis set to approximate the wavefunction. A geometry search restricted to structures with linear and bifurcated hydrogen bonds is performed and the associated potential energy curves are displayed. The minimum energy geometry of the water dimer is found to form a linear hydrogen bond with a hydrogen bond distance of 2.04 Å and a binding energy of 4.84 kcal/mole relative to the monomer (exp. 5.0 kcal/mole). No semistable structures are found. The charge density and charge density difference maps are discussed for the structure with a linear hydrogen bond for different subsystem (water) separations, including the minimum energy geometry. The dipole moment of the dimer is computed to be 1.69 a.u. The shift of the IR bands on hydrogen bond formation is explained qualitatively by comparing the potential energy curves of the hydrogen in the OH-bonds of the monomer and the dimer, and the intensity increase of the fundamental OH-stretching band is computed. The shift of the proton magnetic resonance signal is discussed qualitatively by inspecting the charge density change on hydrogen bond formation, and the average diamagnetic shielding is calculated.

Die Wasserstoffbrückenbindung im dimeren Wasser ist im Rahmen des SCF-MO-LCAO-Verfahrens untersucht worden, wobei die Wellenfunktion durch Gaußfunktionen angenähert wurde. Die Untersuchungen beschränkten sich auf Strukturen mit linearen und „gegabelten" Wasserstoffbrücken. Die zugehörigen Potentialkurven wurden berechnet und graphisch dargestellt. Danach besitzt das dimere Wasser in der energetisch stabilsten Form eine lineare Wasserstoffbrückenbindung mit einem Brückenbindungsabstand von 2,04 Å. Die Bildungsenergie aus zwei monomeren Wassermolekülen beträgt 4,84 Kcal/Mol. Es wurden keine semistabilen Strukturen anderer Geometrie gefunden. Für das dimere Wasser mit linearer Wasserstoffbrückenbindung sind für verschiedene Brückenbindungsabstände die Elektronendichten und die Elektronendichtedifferenzen, bezogen auf zwei ungestörte Wassermoleküle als Vergleichssystem, graphisch dargestellt und diskutiert worden. Das Dipolmoment des dimeren Wassers wurde zu 1,69 a.u. berechnet. Die Verschiebung der IR-Banden, die bei der Bildung der Wasserstoffbrückenbindung experimentell beobachtet wird, kann qualitativ aufgrund der entsprechenden Potentialkurven erklärt werden. Die dabei gleichfalls beobachtete Intensitätszunahme wurde berechnet. Die Verschiebung des Proton-Kernresonanzsignals konnte qualitativ an Hand der berechneten Ladungsdichtedifferenzen diskutiert und die diamagnetische Abschirmkonstante bestimmt werden.

Etude de la liaison hydrogène du dimère de l'eau dans le cadre SCF-MO-LCAO en utilisant une grande base de fonctions gaussiennes. La géométrie est recherchée parmi les structures à liaisons hydrogène linéaires et fourchues avec production des courbes d'énergie potentielle associées. La géométrie du dimère d'énergie minimum est du type liaison hydrogène linéaire de longueur 2,04 Å et d'énergie 4,84 Kcal/mole (exp. 5,0 Kcal/mole). On ne trouve pas de structures semi-stables. Les cartes de densité de charge et de densité différentielle sont discutées pour différentes distances de séparation du système à liaison hydrogène linéaire. Le moment dipolaire du dimère est évalué à 1,69 u.a. Le déplacement des bandes I.R par formation de liaison hydrogène est expliqué qualitativement

* These studies were started while the author was visiting the IBM Research Laboratories, San Jose, California 95114, USA.

en comparant les courbes d'énergie potentielle de la liaison OH dans le monomère et le dimère, et l'on calcule l'augmentation d'intensité de la bande fondamentale de vibration OH. Le déplacement du signal de résonance magnétique du proton est discuté qualitativement par inspection des variations de densité de charge par formation de la liaison hydrogène, et l'on a calculé l'écran diamagnétique moyen.

1. Introduction

The hydrogen bond has been of special interest to chemists since Latimer and Rodebush [1] in 1920 first used this bond mechanism to describe the structure of water. The interest greatly increased when Watson and Crick [2] in 1953 postulated hydrogen bonding to be a key feature of the structure of DNA and when Deryagin and coworkers [3] in 1965 seemed to have discovered a form of anomalous water.

The term "hydrogen bond" has no universally accepted definition. In a most general way Pimentel and McClellen [4] used it to refer to an interaction between a group A–H and an atom or group of atoms B in the same or a different molecule when there is evidence of bond formation and when there is evidence that this new bond, linking A–H and B, specifically involves the hydrogen atom already bonded to A. Of the two functional groups taking part in the interaction, A-H serves as a proton donor and B as an electron donor (or proton acceptor). Most commonly known groups acting as proton donors are: the carboxyl-, hydroxyl-, amine-, or amide group. Moreover the proton attached to carbon, phosphorus, sulfur, selenium and particularly to fluorine can take part in hydrogen bonding. The electron contributing parts of the molecule are usually oxygen in carbonyls, ethers, and hydroxyls, nitrogen in amines and N-heterocyclic compounds and halogen atoms in some molecular environments.

The dissociation energy of hydrogen bonds varies from a few kcal/mole to about 40 kcal/mole depending on the different functional groups envolved. The formation of a hydrogen bond modifies a great many physical and chemical properties. The most common, or most commonly observed, and most characteristic property modifications are: frequency shifts of IR and Raman bands as well as of UV and visible spectra, shifts of proton magnetic resonance signals, altered freezing and boiling points and changed electrical conductivities. The infrared and Raman spectra are characterized by a low frequency shift, with respect to those of the nonbonded molecules, of the AH stretching bands and by an increase of the integrated intensity of the fundamental stretching band. In the ultraviolet spectra both hypsochromic and bathochromic shifts are observed. The $n \rightarrow \pi^*$ transitions are generally displaced to the blue and the $\pi \rightarrow \pi^*$ usually, but not invariably, to the red. Finally, in the nuclear magnetic resonance spectra the proton signal is shifted to lower fields although there are some exceptions to this rule [5].

The early theoretical work on hydrogen bonding was started by Pauling (1928) [6]. It was based on the argument that the hydrogen bond interaction of AH and B can be described by that of the two charge distributions associated with the unperturbed AH and B. Actually, the formation of hydrogen bonds disturbes these distributions and therefore such simple electrostatic theories were only partly able to describe the experimental results [7].

The first quantum mechanical approach to the problem of hydrogen bonding at all was due to Sokolov (1947) and it was based on the valence bond theory. Later a number of studies along the same line were undertaken, marked by the attempt to find the ionic and covalent contributions to the hydrogen bond [7]. Then Pimentel (1951) [9] was the first to apply the molecular orbital theory to hydrogen bonding. Meantime there have been numerous studies on hydrogen bonding by semiempirical molecular orbital methods, as for example by the Hückel and Extended Hückel theory and most recently by the CNDO and NDDO methods [7]. Especially the last two approaches have been applied to a number of hydrogen bonded systems and have given encouraging results [10–17, 46].

With the advent of high speed computers it has become possible to study simple hydrogen bonded systems, taking all electrons into account, by the self-consistent-field method, without any approximations in the integrals. The first investigation of this type was done by Clementi (1961) [18], and by Clementi and McLean [19] on the bifluoride ion FHF^- [51]. Since then a number of studies have been reported on the system $NH_3 + HCL$ [20], as well as on the systems $(NH_3)_2$ [50], $(H_2O)_2$ and higher polymers [21–26, 55, 47–49], $(HF)_2$ and higher polymers [48, 49, 52], NH_3H_2O [50], NH_3HF [50], H_2OHF [48], $H_2OHOH_2^+$ [28, 51], $HOHOH^-$ [53], $HOHF^-$ [27], $HOHFHOH^-$ [57], $(HCOOH)_2$ [58], guanine and cytosine [58].

In the present paper an SCF-MO-LCGO study on dimeric water will be presented, using a large gaussian basis set. The hope was to get more accurate information about parts of the energy hypersurface, about the minimum energy geometry, and about a number of properties than available from calculated SCF-wavefunctions so far [21–26, 47–49].

2. Method of Calculation and Description of Basis Set

The wavefunctions and energies reported are calculated using Roothaan's SCF-LCAO-MO method [29]. The computations are carried out with the program system IBMOL/VERSION IV [30], modified by the author (GD) to avoid the explicit integral transformation [31]. The properties discussed have been computed by a program package originally written at the New York University [32] and amended for use on the computer series IBM 360 [33]. All calculations have been carried out on an IBM 360/91 computer.

The molecular orbitals ϕ which are used in building up the total wavefunction of the single determinant Hartree-Fock method are expanded into a set of basis functions consisting of uncontracted Gaussian functions χ and contracted Gaussian functions χ', according to the following equation:

$$\phi = \sum_k c_k \chi_k + \sum_l c'_l \chi'_l . \tag{1}$$

The uncontracted (or primitive) Gaussian functions (GTO's) are of the form:

$$\chi_k = N_k f_k(x, y, z) \exp(-\alpha_k r^2), \tag{2}$$

where x, y, and z are Cartesian Coordinates relative to the function's center. The prefactor $f(x, y, z)$ is 1 for s-type GTO's; x, y, or z for p-type GTO's; and x^2, y^2,

z^2, xy, xz, or yz for d-type GTO's. The contracted Gaussian functions (CGF's) consist of linear combinations of GTO's according to Eq. (3):

$$\chi_l' = N_l \sum_m a_m \chi_m \,. \tag{3}$$

The set of GTO's into which a particular CGF is expanded is constrained to have the same center and to be of the same type. These limitations allow the form of the CGF's in (3) to be simplified to

$$\chi_l' = N_l' f_l(x, y, z) \sum_n a_n \exp(-\alpha_n r_n^2) \,. \tag{4}$$

Thus, a CGF is completely determined by its type, its center, a set of exponents α_n, and a set of coefficients a_n.

The molecular orbitals for the wavefunctions to be reported here are all expanded into the same Gaussian bais set, chosen from the set published by Veillard [34], and extended by a d-type polarization function at the oxygen and a p-type polarization function at the hydrogen to increase the flexibility of the wavefunction in describing the valence electrons. The uncontracted basis set, denoted by (1171/61) [35], is made up of 11s-, 7p-, and 1d-type GTO's at the oxygen (1171) and by 6s-, and 1p-type GTO's at the hydrogen (61). The contracted basis set in term, denoted by [541/31], is formed by contracting the (1171/61) GTO set to 5s-, 4p-, and 1d-type CGF's at the oxygen [541], and to 3s-, and 1p-type CGF's at the hydrogen [31]. The exponents for the d-type GTO at the oxygen and the p-type GTO at the hydrogen are optimized by self-consistent-field calculations within the framework of the above basis set on the experimental geometry configuration of water. – The Gaussian basis set for oxygen and hydrogen are given in Table 1.

Computations on the water molecule will be presented first. There are many experimental data and a series of theoretical investigations [39] available on this molecule to study the accuracy of the computed wavefunctions, expanded into the basis set as described. Moreover, some of the results of the monomer are necessary for comparison with the results to be computed for the dimer later.

A search for the minimum energy geometry of water has been made by varying the bond distance d(OH), keeping the bond angle α(HOH) fixed, and vice versa. The total SCF energy for different values of the parameters d(OH) and α(HOH) is given in Table 2. By interpolating between the three lowest points in energy, using a parabolic approximation, the minimum energy configuration was found to have a bond distance of $d(\mathrm{OH}) = 0.9443$ Å (exptl. 0.9572 Å), a bond angle of $\alpha(\mathrm{HOH}) = 105.33°$ (exptl. 104.52°) and a total SCF energy of $E^{\mathrm{SCF}} = -76.05326$ a.u. The computed bond distance and bond angle compares nicely with the experimental values. The total SCF energy is off by 0.007 a.u. from the best calculated value known (– 76.05936 a.u. [36]) which in turn is believed to be off by 0.01 to 0.03 a.u. from the Hartree-Fock limit [36].

For the experimental geometry configuration of water ($d(\mathrm{OH}) = 0.9572$ Å, $\alpha(\mathrm{HOH}) = 104.52°$) a number of results are listed: the molecular orbital energies and coefficients are compiled in Table 3. The results computed for some different expectation values are edited in Table 4. The experimental data, if available,

Table 1. *Gaussian basis set for oxygen and hydrogen*

Center	Type	CGF Nr.	CGF Coefficients *a*	GTO Exponents α
O	*s*	1	0.001437	18045.300000
			0.011513	2660.120000
			0.062186	585.663000
			0.251624	160.920000
			0.752696	51.163700
		2	0.558935	17.896600
			0.484098	6.639010
		3	1.000000	2.096250
		4	0.572456	0.842082
			0.471727	0.307280
		5	1.000000	0.132539
	p	1	0.016459	49.827900
			0.106183	11.488700
			0.353659	3.609240
			0.654088	1.311040
		2	1.000000	0.502347
		3	1.000000	0.195677
		4	1.000000	0.072412
	d	1	1.000000	1.000000
H	*s*	1	0.023654	68.160000
			0.179767	10.246500
			0.860803	2.346480
		2	0.392415	0.673320
			0.656304	0.224660
		3	1.000000	0.082217
	p	1	1.000000	0.750000

Table 2. *Total* SCF *energies for water for different nuclear geometries*[a]

	$d(OH_1)$ [Å]	$d(OH_2)$ [Å]	α(HOH)	*E*(SCF) [a.u.]
1	0.8800	0.8800	104.52°	−76.042016
2	0.9000	0.9000	104.52°	0.047697
3	0.9200	0.9200	104.52°	0.051033
4	0.9400	0.9400	104.52°	0.052322
5	0.9572	0.9572	104.52°	0.051990
6	0.9800	0.9800	104.52°	0.049759
7	1.0200	1.0200	104.52°	0.041731
8	0.9572	0.8800	104.52°	−76.046959
9	0.9572	0.9200	104.52°	0.051502
10	0.9572	0.9800	104.52°	0.050871
11	0.9572	1.0200	104.52°	0.046831
12	0.9572	0.9572	100°	−76.051264
13	0.9572	0.9572	108°	0.051821

[a] Geometry parameters are defined in Fig. 1.

Table 3. *Molecular orbital energies and coefficients for water*[a, b]

Orbital number		1	2	3	4	5
Symmetry type		$1A1$	$2A1$	$1B2$	$3A1$	$1B1$
Energy		−20.56600	−1.35322	−0.72035	−0.58455	−0.51059
Coefficients						
Center	Type					
O	s	0.28952	−0.06090	0.00000	0.02033	0.00000
		0.75898	−0.24224	0.00000	0.08166	0.00000
		0.05589	−0.07451	0.00000	0.03078	0.00000
		0.01026	1.06868	0.00000	−0.43796	0.00000
		0.00372	−0.12173	0.00000	−0.17203	0.00000
	p_x	0.00191	−0.06426	0.00000	−0.43655	0.00000
		0.00264	−0.06793	0.00000	−0.31484	0.00000
		0.00037	0.02084	0.00000	−0.16918	0.00000
		0.00025	0.01932	0.00000	−0.03345	0.00000
	p_y	0.00000	0.00000	0.00000	0.00000	0.49856
		0.00000	0.00000	0.00000	0.00000	0.36403
		0.00000	0.00000	0.00000	0.00000	0.26688
		0.00000	0.00000	0.00000	0.00000	0.06370
	p_z	0.00000	0.00000	0.39420	0.00000	0.00000
		0.00000	0.00000	0.29558	0.00000	0.00000
		0.00000	0.00000	0.06165	0.00000	0.00000
		0.00000	0.00000	0.06422	0.00000	0.00000
	d_{xx}	0.00044	−0.04965	0.00000	0.04154	0.00000
	d_{xy}	0.00000	0.00000	0.00000	0.00000	−0.02058
	d_{xz}	0.00000	0.00000	−0.04093	0.00000	0.00000
	d_{yy}	0.00120	−0.06911	0.00000	0.00288	0.00000
	d_{yz}	0.00000	0.00000	0.00000	0.00000	0.00000
	d_{zz}	0.00014	−0.04314	0.00000	0.01722	0.00000
H_1	s	0.00022	0.04827	0.07000	0.04137	0.00000
		0.00200	0.14029	0.33467	0.21497	0.00000
		−0.00130	0.02248	−0.07146	0.01796	0.00000
	p_x	0.00049	0.00819	0.01846	−0.01194	0.00000
	p_y	0.00000	0.00000	0.00000	0.00000	0.03014
	p_z	−0.00088	−0.01396	−0.00976	−0.02195	0.00000
H_2	s	0.00022	0.04827	−0.07000	0.04137	0.00000
		0.00200	0.14029	−0.33467	0.21497	0.00000
		−0.00130	0.02248	0.07146	0.01796	0.00000
	p_x	0.00049	0.00819	−0.01846	−0.01194	0.00000
	p_y	0.00000	0.00000	0.00000	0.00000	0.30140
	p_z	0.00088	0.01396	−0.00976	0.02195	0.00000

[a] Geometry parameters are defined in Fig. 1; $d(\mathrm{OH}) = 0.9572$ Å, and $\alpha(\mathrm{HOH}) = 104.52°$.
[b] Orbital energies in a.u.

and the results obtained by Neumann and Moskowitz [36] from two wavefunctions expanded in large Gaussian type basis sets are listed in Table 4 as well.

The dipole moment is about 20% greater than the experimental value; the second and quadrupole moments agree reasonably with the values computed from the (1062/41) and [532/21] basis set wavefunctions of Neumann and Moskowitz. The diamagnetic susceptibility is approx. 6% greater than the experi-

Table 4. *Calculated properties of water*[a]

Property[b]		Total 541/31	Total [36] (1062/42)	Total [36] 532/21	Exptl.
Dipole moment	μ(O)	0.8680	0.7850	0.8230	0.728 [37]
Second moment[c]	$Q(\mathrm{CM})_{xx}$	− 4.4980	− 4.4160	− 4.3390	
	$Q(\mathrm{CM})_{yy}$	− 5.6200	− 5.5630	− 5.4690	
	$Q(\mathrm{CM})_{zz}$	− 3.1890	− 3.1080	− 3.0500	
Diamagnetic susceptibility[c]	$\langle r^2\rangle$(CM)	19.4600	19.1810	18.9520	18.3 ± 2.4 [38]
Quadrupole moment[c]	$\Theta(\mathrm{CM})_{xx}$	− 0.0942	− 0.0805	− 0.0788	
	$\Theta(\mathrm{CM})_{yy}$	− 1.7760	− 1.8010	− 1.7760	
	$\Theta(\mathrm{CM})_{zz}$	1.8710	1.8820	1.8550	
Potential	ϕ(O)	− 22.3320	− 22.3340	− 22.3290	
	ϕ(H)	− 0.9930	− 1.0010	− 1.0070	
Diamagnetic shielding	σ^d_{AV}(H)[d]	102.3000	102.9000	103.0000	102.12 [36]
Electric field	$E(\mathrm{O})_x$	0.0730	0.0100	0.0600	
	$E(\mathrm{H})_x$	0.0060	0.0020	0.0010	
	$E(\mathrm{H})_z$	0.0140	0.0000	0.0070	
Charge density	$\langle\delta(r-\mathrm{O})\rangle$	299.6840	299.4970	286.4890	
	$\langle\delta(r-\mathrm{H})\rangle$	0.4350	0.3920	0.4050	
Field gradient	$q(\mathrm{O})_{xx}$	− 0.1930	− 0.1730	− 0.1690	
	$q(\mathrm{O})_{yy}$	1.8980	1.8520	1.9050	
	$q(\mathrm{O})_{zz}$	− 1.7050	− 1.6790	− 1.7360	
	$q(\mathrm{D})_{x'x'}$[e]	0.2180	0.2250	0.2300	
	$q(\mathrm{D})_{yy}$	0.2850	0.2940	0.3010	
	$q(\mathrm{D})_{z'z'}$[e]	− 0.5030	− 0.5190	− 0.5310	
	$q(\mathrm{D})_{x'z'}$[e]	0.0000	0.0000	0.0000	
Quadrupole coupling constants	$qu(\mathrm{O})_{xx}$[f]	− 1.0900	− 0.9750	− 0.9530	2.92 [36]
	$qu(\mathrm{O})_{yy}$[f]	10.7000	10.4400	10.7400	6.96
	$qu(\mathrm{O})_{zz}$[f]	− 9.6100	− 9.4700	− 9.7900	− 9.88
	η(O)	0.7960	0.8130	0.8230	1.84
	$qu(\mathrm{D})_{x'x'}$[e,g]	− 144.2000	− 149.1000	− 152.4000	− 140 ± 7 [36]
	$qu(\mathrm{D})_{yy}$[g]	− 188.8000	− 194.8000	− 199.4000	− 175 ± 10
	$qu(\mathrm{D})_{z'z'}$[e,g]	333.3000	343.9000	351.8000	315 ± 7
	η(D)	0.1340	0.1330	0.1340	0.115 ± 0.061
	ϕ(D)	0.87°	0.97°	0.70°	1°7′ ± 47′

[a] All values in a.u., unless stated otherwise.
[b] For a definition of the expectation values, see [36].
[c] Values relative to the center of mass.
[d] Values in ppm.
[e] The principal axis x' and z' are defined in Fig. 1.
[f] Values in Mc/sec.
[g] Values in kc/sec.

mental value. In general, the multipol moments computed with the [541/31] basis set wavefunction are not as close to the experimental values as those computed from the (1062/42) and [532/21] basis set wavefunctions. This is most likely due to the smaller flexibility of the [541/31] basis set in describing the pola-

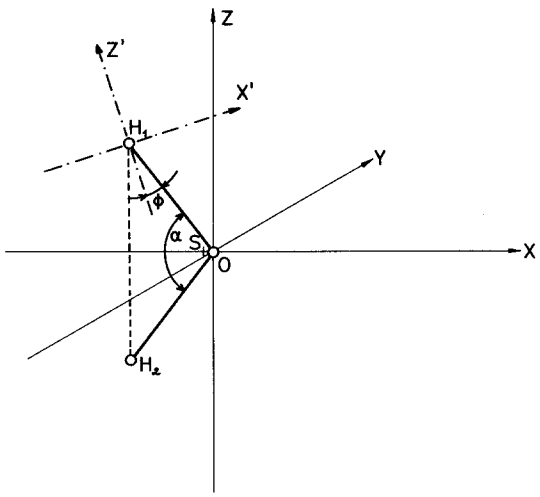

Fig. 1. Coordinate system for water

rization effects, which is dependent on the number and form of the polarization functions included in the basis set (in this case d_O and p_H type GTO's).

The potential and diamagnetic shielding are relatively insensible to the accuracy of the wavefunction, because both are dependent on $1/r$ which plays an important role in the Hamiltonian. Therefore they can be expected to be reasonably accurate; this is supported by the good agreement of computed and experimental values for the diamagnetic shielding.

The electric field at oxygen and hydrogen can be used to compute the force on the nuclei, which is equal to the electric field times the nuclear charge. The Hellmann-Feynmann theorem predicts, that the sum of all forces on all the nuclei should be zero for a Hartree-Fock wavefunction at the experimental equilibrium geometry. In addition, the net force on each nucleus should be zero. It is seen that these conditions are not fulfilled for the wavefunctions discussed. It is not known how much of the residual forces are due to a slightly incorrect geometry and how much to the incompletely optimized wavefunctions.

The quadrupole coupling constants of deuterium, depending primarily on the charge distribution near the oxygens, agree within 5–7% with the experimental values, the error being only slightly greater than the experimental uncertainty. The quadrupole coupling constants of oxygen, depending on the more spred out charge distribution, which shows the greater inaccuracies, are in less good agreement with the experiment.

This study of the water molecule shows, that the geometry parameters and the properties listed in Table 4 (except the quadrupole coupling constants for oxygen) agree reasonably well with the experimental data, in cases where a comparison is possible, and with the values computed from the (1062/42) and [532/21] basis set wavefunctions of Neuman and Moskowitz. For an investigation of a system of two interacting water molecules a wavefunction with its molecular

orbitals expanded into the [531/31] basis set therefore was felt to be adequate. The geometry parameters and the molecular properties of the dimeric system are expected to be of comparable accuracy.

3. Two Interacting Water Molecules

So far a number of *ab initio* studies on two interacting water molecules have been published [21–26, 47–49]. The most interesting features of these investigations are collected in Table 5: the basis set type and size, the minimum energy geometry parameters including the OH bond stretching on hydrogen bond formation, and the associated SCF-energy and binding energy. Summarizing the results it seems to be well established that in the minimum energy geometry the interaction of the two molecules is through a linear hydrogen bridge with an oxygen-oxygen distance of approximately $d(O_1O_2) = 3.00$ Å and a binding energy between 4.5 and 6.5 kcal/mole. There is no agreement about the geometry parameter ϑ which varies between 0° and 58°. The computed O_2H_3 bond stretching is extremely small. In the following the results obtained by the present study will be discussed.

Geometry Search and Energy Hypersurface

The geometry search has been limited to those structures where the proton or the protons are donated by only one of the two water molecules under consideration (Fig. 2). So called "cyclic" structures where both water molecules are acting as a donor of one proton and an acceptor of another proton simultaneously are not considered here. The investigation of Morokuma and Pedersen [21] as well as of Kollman and Allen [22] have shown that these structures are highest in energy (smallest binding energy) when the interaction of only two water molecules is considered.

A system of two water molecules approaching each other with one hydrogen atom positioned on the line connecting the two oxygen atoms, and the planes of the two water molecules perpendicular to each other – linear perpendicular geometry – has been studied first. In this system the interaction is through a *single linear* hydrogen bridge. The geometry parameters of the individual water molecules have been kept at their experimental values of $d(OH) = 0.9752$ Å and $(HOH) = 104.52°$ throughout this investigation, unless stated otherwise. The energy curve has been computed over a wide range of oxygen-oxygen distances and is displayed in Fig. 3. The numerical results are listed in Table 6, lines 1 through 21.

The minimum total SCF-energy of $E^{SCF} = -152.11167$ a.u. was found for an oxygen-oxygen distance $d(O_1O_2) = 3.00$ Å. According to the results reported for the water molecule, it is believed that the total energy for the dimeric water is off by 0.04 to 0.08 a.u, from the Hartree-Fock value. A fine grid of points has been chosen around the energy minimum. Although most of the values computed for this region differ by a few figures on the 5. decimal place only, all values are in the expected order. Because the energy curve is very flat near the minimum the oxygen-oxygen distance is most likely uncertain by about ± 0.025 Å.

Table 5. *Comparison of results obtained by different "ab initio" calculations on dimeric water*

	Basis set	Equil. $d(O_1O_2)$ [Å][a]	Equil. ϑ[a]	$\Delta d(O_2H_3)$ [Å][a,b]	Min. E^{SCF} [a.u.]	Bind. energy [kcal/mole]	References
1	Small GTO	2.68	0°	0.0120	−151.123350	−12.60	Morokuma and Pedersen [21]
2	Med. size GTO, no polariz. fct.	3.00	25°	0.0100	−151.957680	− 5.30	Kollman and Allen [22]
3	Minimal STO	2.73	58°	—	−151.009980	− 6.09	Del Bene and Pople [24, 47]
4	Extended double ζ-GTO	3.00	40°	—	—	− 4.72	Hankins, Moskowitz and Stillinger [25]
5	Minimal STO	2.78	53.8°	0.0026	−151.420506	− 6.55	Morokuma and Winick [26]
6	Extended double ζ-GTO	3.00	?	0.0040	−152.111670	− 4.84	This paper

[a] Geometry parameters are defined in Fig. 2; $\psi = 52.26°$, $\varphi = 0°$.

[b] Positive values for OH bond stretching.

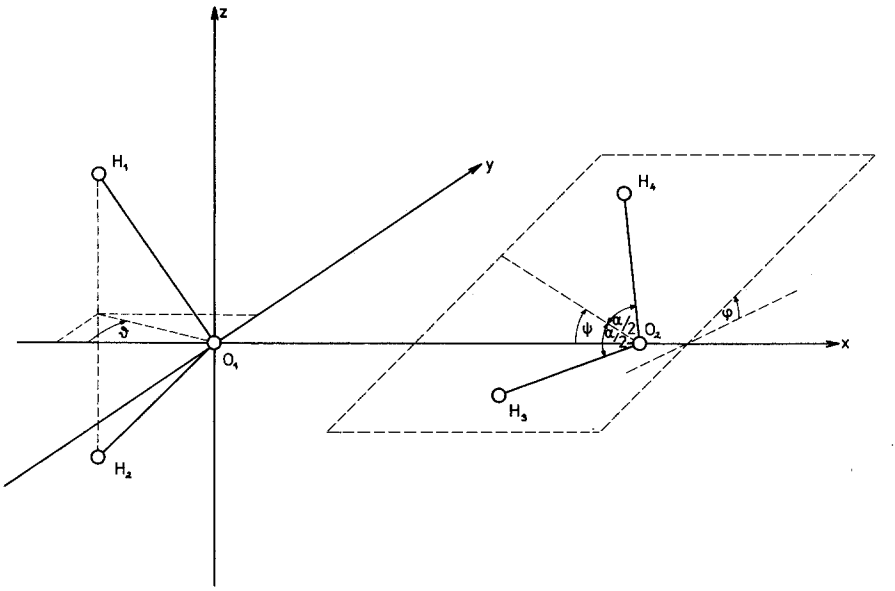

Fig. 2. Coordinate system for dimeric water

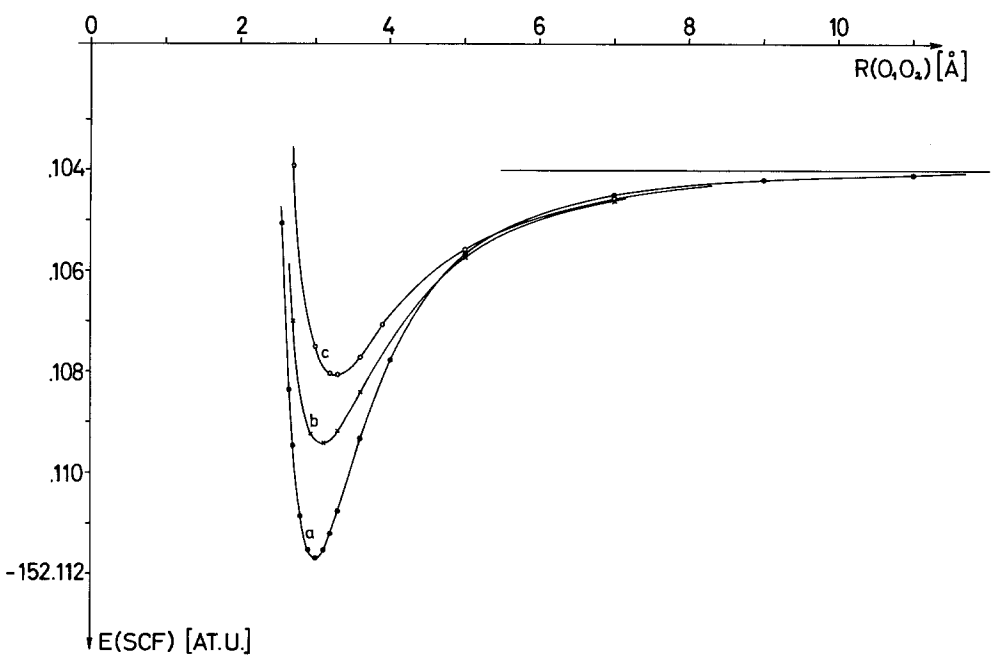

Fig. 3. Energy curves for dimeric water: a) linear perpendicular geometry; b) bifurcated perpendicular geometry; c) bifurcated planar geometry

Table 6. *Total* SCF-*energies for dimeric water for different nuclear geometries*[a]

	$R(O_1O_2)$ [Å]	R(OH) [Å]	$R(O_2H_3)$ [Å]	α [degree]	φ	ψ	ϑ	E(SCF) [a.u.]
1	2.55	0.9572	0.9572	104.52	0	52.26	0	−152.10509
2	2.65							0.10836
3	2.70							0.10946
4	2.75							0.11027
5	2.80							0.11086
6	2.85							0.11126
7	2.90							0.11152
8	2.95							0.11165
9	3.00							0.11167
10	3.05							0.11164
11	3.10							0.11153
12	3.15							0.11138
13	3.20							0.11120
14	3.25							0.11090
15	3.30							0.11077
16	3.60							0.10932
17	4.00							0.10773
18	5.00							0.10569
19	7.00							0.10450
20	9.00							0.10421
21	11.00							0.10410
22	3.00	0.9572	0.9572	104.52	90	52.26	0	−152.11126
23	3.00	0.9572	0.9040	104.52	0	52.26	0	−152.10954
24			0.9310					0.11144
25			0.9840					0.11052
26			1.0100					0.10820
27			1.1690					0.07918
28			1.3810					0.02768
29			1.5920					−151.98461
29a		0.9300	0.9300					−152.11152
29b		0.9800	0.9800					0.10914
30	7.00	0.9572	1.1700	104.52	0	52.26	0	−152.10398
31			1.3800					0.09842
32			1.5900					−151.95901
33			1.8100					0.91128
34			6.0200					0.80498
35	2.30	0.9572	1.1500	104.52	0	52.26	0	−152.05339
36	3.00	0.9572	0.9572	109.28	0	54.73	10	−152.11125
37							20	0.11137
38							30	0.11146
39							40	0.11148
39a							59.73	0.11128
40	2.70	0.9572	0.9572	104.52	90	0	0	−152.10699
41	3.00							0.10751
42	3.20							0.10804
43	3.30							0.10806
44	3.60							0.10772
45	3.90							0.10718
46	5.00							0.10562
47	7.00							0.10460

Table 6 (continued)

	$R(O_1O_2)$ [Å]	$R(OH)$ [Å]	$R(O_2H_3)$ [Å]	α [degree]	φ	ψ	ϑ	E(SCF) [a.u.]
48	2.65	0.9572	0.9572	104.52	0	0	0	−152.10699
49	2.95							0.10923
50	3.12							0.10943
51	3.30							0.10918
52	3.60							0.10841
53	5.00							0.10573
54	7.00							0.10462
55	3.18	0.9572	0.9572	104.52	30	0	0	−152.10905
56	3.24				60			0.10838
57	3.046	0.9572	0.9572	104.52	0	32.26	0	−152.11085
58	3.092					12.26		0.10968

(Some additional results are given in Table 10.)

[a] Geometry parameters are defined in Fig. 2.

Next the total SCF-energy has been computed at an oxygen-oxygen separation of $d(O_1O_2) = 3.00$ Å for the geometry with the linear hydrogen bond and the two water molecules in the same plane – linear planar geometry. The value was calculated to be $E^{SCF} = -152.11126$ a.u. (Table 6, line 22). This is about 0.26 kcal/mole higher than the total SCF-energy computed for the linear perpendicular geometry. It indicates effectively free rotation of the two interacting molecules around the hydrogen bond axis (x-axis), although only two points have been studied.

In some modifications of ice each oxygen atom is acting as donor of two protons and acceptor of two different protons in such a way that the four "bonds" of the oxygen atoms form approximately tetrahedral angles [40].

The geometry which two water molecules are known to have in ice may be a competitive form for the minimum energy structure of the dimer.Therefore the total SCF-energy change has been analyzed for the linear structure, at $d(O_1O_2) = 3.00$ Å, fixing the angle φ to $\varphi = 0$, the angle $\alpha(H_1O_1H_2)$ to $\alpha = 109.28°$ and varying the angle ϑ from $\vartheta = 10°$ to $\vartheta = 54.73°$. The potential energy curve is displayed in Fig. 4, and the numerical values are listed in Table 6, lines 36 through 39a. An energy minimum is found for an angle between $\vartheta = 35°$ and $\vartheta = 40°$ with the total energy about 0.12 kcal/mole higher than the energy computed for the linear perpendicular structure at the same oxygen-oxygen separation. Due to the lack of grid points, the detailed behaviour of the energy curve is uncertain and has not been plotted in the region of the energy barrier (approx. $\vartheta = 3°$ to $\vartheta = 10°$). The energy barrier itself may reasonably be estimated to be about 0.3 kcal/mole.

For molecular calculations the wavefunctions have to be expanded in basis sets of finite and especially of handable size, therefore they are mathematically not complete. For this reason the approximated wavefunctions may not be flexible enough to represent the charge distribution equally well for different geometrical configurations of a system. This eventually will give rise to errors which

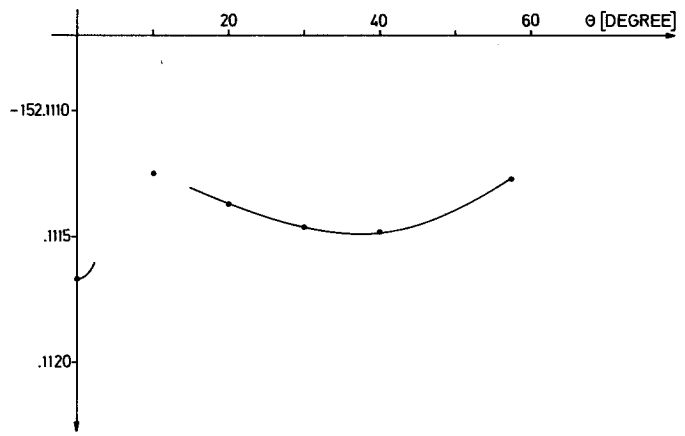

Fig. 4. Energy curve for dimeric water in the linear geometry at an oxygen-oxygen separation of $d(O_1O_2) = 3.00$ Å

may falsicate the energy dependence on geometrical parameters. In the MO-LCAO-approximation, the energy dependence on "radial" parameters, relative to a constituent center, may be rather well described, while functions with higher quantum numbers have to be included in the basis set when analyzing the energy dependence on "angular" parameters.

The double minimum of the potential energy hypersurface of the system under consideration, with an energy barrier of about 0.3 kcal/mole may well be a physical characteristic of the molecular system discussed. But with the above considerations in mind no reasonable decision is possible here about which of the two minima is the absolute one, defining the minimum energy geometry. A more detailed discussion of this point must include a variation of the oxygen-oxygen distance and the angle $\alpha(H_1O_1H_2)$ for each angle ϑ.

The change in energy for a system of two water molecules approaching each other in a way that two symmetrical hydrogen bonds can be formed – bifurcated geometry – has been studied as well. Those systems interact through *two* protons donated by *one* of the water molecules. The bifurcated structures have been examined for the two water molecules approaching each other with their planes planar ($\varphi = 90°$) and perpendicular ($\varphi = 0°$) to each other. The computed energy curves are displayed in Fig. 3, and the numerical results are listed in Table 6, lines 40 to 54. The minimum total SCF-energies have been computed to be $E^{SCF} = -152.1081$ a.u. and $E^{SCF} = -152.1094$ a.u. for the planar and perpendicular geometry, resp. The associated oxygen-oxygen distances are calculated to be $d(O_1O_2) = 3.33$ Å and $d(O_1O_2) = 3.12$ Å, resp. These distances are determined by a parabula approximation from the results listed, using for each geometry the three lowest points in energy.

By simple rotation of one of the constituent water molecules the linear and bifurcated structure of dimeric water can be transferred into each other. In order that the bifurcated structures are semistable systems they have to be separated from each other and from the linear structure by energy barriers. A

number of calculations are undertaken to clear up this question. The numerical results are listed in Table 6, lines 55 to 58. It was found that no such energy barriers exist along the "path" tested. Thus the linear structure is the only stable system of two interacting water molecules.

An equilibrium oxygen-oxygen distance of $d(O_1O_2) = 3.00$ Å was computed for the linear perpendicular structure of two interacting water molecules, the stable form. This corresponds to a hydrogen bond length of $d(O_1H_3) = 2.04$ Å. For dimeric water in the gas phase there are no experimental data available for comparison. The observed values of the oxygen-oxygen distance in cubic and hexagonal ice are $d(O_1O_2) = 2.74$ Å and $d(O_1O_2) = 2.77$ Å, resp. [40]. The computed hydrogen bond distance in the dimer is about 10% larger than the experimental value measured in the crystal. This seems to be rather astonishing because one should expect a smaller hydrogen bond length in the dimer than in the higher polymers (crystals, chains, rings) because of the additional steric crowding effect which can be expected to increase the "inter-molecular" bond length in the polymers. This implies that in the calculations on the dimer important characteristic features that are of effect on the bonding in the polymers have not been taken into account. Therefore the results obtained by calculations on the dimer cannot be generalized easily to polymers of water.

The energy differences between the linear and bifurcated structures of dimeric water are very small (less than one kcal/mole). Therefore neighbouring effects may be of influence on the geometry of dimeric water other than in the gas phase (where it is practically an isolated system) and different geometries have to be expected under different conditions. The many different structures of ice seem to support this.

Binding Energy

Fair estimates of the binding energy may be found from SCF-calculations, using wavefunctions approximated by extended basis sets. The values derived are known to be in reasonable agreement with experiment, if the break of the chemical bond to be considered does involve no or only small changes in the correlation energy. This seems usually to be true for systems that dissociate into parts with even numbers of electrons (closed shell systems) as, for example, in dimeric water.

The binding energy is defined as the difference between the sum of the minimum energies of the subsystems and the minimum energy of the bonded system. Before comparing the binding energy to the observed dissociation energy, the latter has to be corrected by adding the so-called zero point energy due to the lowest possible vibrational state in the appropriate molecular system. For diatomic systems, the zero point energy is easy to compute, for polyatomic systems it is very troublesome. Therefore, very often the binding energy is compared directly to the dissociation energy. In the example under consideration this should be a good approximation, because the potential energy curve for the hydrogen bond is very flat and the change of the zero point energy can be expected to be small.

The binding energy computed in this way for the hydrogen bond of dimeric water in the linear configuration is $B = 4.83$ kcal/mole. For the planar bifurcated

configuration the hydrogen binding energy was found to be $B = 2.59$ kcal/mole and for the perpendicular $B = 3.42$ kcal/mole.

The binding energy of $B = 4.83$ kcal/mole, calculated for the stable geometrical configuration, agrees favourably with the experimental value of 5.0 kcal/mole for the water dimer in the gas phase and of 5.7 kcal/mole per hydrogen bond in ice [4].

Wavefunction and Charge Distribution

The molecular orbital coefficients and -energies are given in Table 7 for the minimum energy geometry of dimeric water[1]. In addition the orbital energies are listed for a number of different distances $d(O_1O_2)$ for the linear perpendicular geometry in Table 8. In the following discussion it is well understood that molecular orbitals and -energies do not have too much meaning by itself. Both are not invariant under unitary transformations which leave the *total* energy and the *total* electron density unchanged.

The orbitals localized at the proton acceptor molecules are always found to be lower in energy and those localized at the proton donor are always found to be higher in energy than the comparable molecular orbitals of the isolated water molecule [22]. From the highest orbital energy the ionisation energy is calculated according to Koopman's theorem [41] to be 13.06 eV for dimeric water and to be 13.84 eV for monomer water. Thus the dimeric water has a ionisation energy of about 0.78 eV lower than the monomer. For large separations of the water molecules the orbital energies are converging pairwise against the values computed for the monomer. This indicates that dimeric water separates "properly" into the two constituent water molecules and that a correct behaviour of the wavefunction can be expected.

The molecular orbital coefficients are very hard to interprete by themselves. Therefore, charge density contour lines have been computed and are displayed in Fig. 5a for the xz-plane, and in Fig. 5b for the xy-plane. The orbitals 1 through 4 are localized at the two oxygen atoms and are of 1s- and 2s-type, resp. They do not take part in the chemical bonding and, therefore, are not included in the figures. The total electron density of orbitals 5 through 10 gives no unique indication of a charge shift in dimeric water relative to the charge distribution expected for two non-interacting water molecules. Electron density contour lines of the individual orbitals are displayed as well and it may be worthwhile to analyze them: all orbitals are very much localized at the "originating" water molecules. Small contributions localized at the "other" water molecules mix in for orbitals 6 through 9. These four orbitals are those which are most polarized by the interaction of the two molecules and which, therefore, may be said to make the greatest contribution to the hydrogen bond.

Electronic density differences have been found especially useful if small charge density changes have to be analysed. They are defined as the difference of the charge distribution computed for the total system and the charge densities computed for the reference systems. Density difference contour lines have been calculated

[1] Wave functions for most of the geometries listed in Table 5 are available on request.

Table 7. *Molecular orbital energies and coefficients for dimeric water*[a, b]

Orbital number		1	2	3	4	5	6	7	8	9	10
Energy		−20.59077	−20.53238	−1.37911	−1.32183	−0.74492	−0.69553	−0.61539	−0.55121	−0.53633	0.47945
Orbital Coefficients											
Center	Type										
O_1	s	−0.28952	−0.00001	0.06091	0.00381	0.00000	−0.00389	−0.01816	0.00593	0.00057	0.00000
		−0.75895	−0.00008	0.24209	0.01538	0.00000	−0.01559	−0.07295	0.02389	0.00231	0.00000
		−0.05613	0.00043	0.07693	0.00214	0.00000	−0.00570	−0.02829	0.00909	0.00043	0.00000
		0.01075	−0.00100	−1.07434	−0.05974	0.00000	0.08578	0.39028	−0.12556	−0.01050	0.00000
		−0.00404	0.00029	0.12449	−0.00831	0.00000	0.03491	0.15247	−0.05529	−0.01179	0.00000
	p_x	0.00178	0.00003	0.06186	0.00742	0.00000	0.11877	0.40493	−0.11013	−0.01178	0.00000
		−0.00245	−0.00011	0.06183	0.00946	0.00000	0.08908	0.29420	−0.07707	−0.00721	0.00000
		0.00008	0.00035	−0.01907	−0.01394	0.00000	0.03218	0.17380	−0.06280	−0.00762	0.00000
		0.00047	−0.00136	−0.00386	−0.01853	0.00000	0.03380	0.06110	−0.02734	−0.00717	0.00000
	p_y	0.00002	0.00000	0.00026	−0.00003	0.00000	0.00265	−0.00801	−0.08045	0.49224	0.00000
		−0.00001	0.00002	0.00028	−0.00011	0.00000	0.00173	−0.00606	−0.05970	0.36028	0.00000
		0.00000	−0.00003	0.00064	0.00064	0.00000	0.00156	−0.00421	−0.04012	0.26454	0.00000
		0.00001	0.00005	−0.00058	−0.00229	0.00000	−0.00143	−0.00310	−0.01533	0.06077	0.00000
	p_z	0.00000	0.00000	0.00000	0.00000	0.39619	0.00000	0.00000	0.00000	0.00000	−0.00493
		0.00000	0.00000	0.00000	0.00000	0.29977	0.00000	0.00000	0.00000	0.00000	−0.00258
		0.00000	0.00000	0.00000	0.00000	0.06442	0.00000	0.00000	0.00000	0.00000	−0.00240
		0.00000	0.00000	0.00000	0.00000	0.07468	0.00000	0.00000	0.00000	0.00000	0.02311
	d_{xx}	−0.00055	0.00022	0.05051	0.00168	0.00000	−0.00763	−0.03658	0.01191	0.00110	0.00000
	d_{xy}	0.00000	0.00000	0.00003	−0.00001	0.00000	−0.00007	−0.00005	0.00280	−0.01848	0.00000
	d_{xz}	0.00000	0.00000	0.00000	0.00000	−0.04022	0.00000	0.00000	0.00000	0.00000	0.00091
	d_{yy}	−0.00130	0.00023	0.07017	0.00385	0.00000	0.00088	−0.00381	0.00229	−0.00028	0.00000
	d_{yz}	0.00000	0.00000	0.00000	0.00000	−0.00020	0.00000	0.00000	0.00000	0.00000	0.00000
	d_{zz}	−0.00025	0.00018	0.04495	0.00121	0.00000	−0.00335	−0.01772	0.00549	0.00023	0.00000

Table 7 (continued)

Orbital number		1	2	3	4	5	6	7	8	9	10
Energy		−20.59077	−20.53238	−1.37911	−1.32183	−0.74492	−0.69553	−0.61539	−0.55121	−0.53633	−0.47945
Orbital Coefficients											
Center	Type										
O_2	s	0.00002	−0.28953	0.00348	−0.06083	0.00000	0.00069	0.00696	0.01845	0.00325	0.00000
		0.00002	−0.75889	0.01361	−0.24148	0.00000	0.00253	0.02781	0.07431	0.01307	0.00000
		0.00026	−0.05685	0.00734	−0.07993	0.00000	0.00390	0.01180	0.02587	0.00518	0.00000
		−0.00057	0.01244	−0.06855	1.08138	0.00000	−0.02046	−0.14843	−0.39174	−0.07035	0.00000
		−0.00006	−0.00600	0.04134	−0.16920	0.00000	0.02315	−0.01113	−0.19847	−0.03541	0.00000
	p_x	−0.00002	0.00115	0.00385	−0.03842	0.00000	−0.30536	0.04462	−0.27767	−0.04429	0.00000
		0.00008	−0.00188	0.00422	−0.04512	0.00000	−0.22721	0.03305	−0.20257	−0.03293	0.00000
		0.00004	0.00077	−0.01084	0.02877	0.00000	−0.05733	−0.00676	−0.09904	−0.01637	0.00000
		0.00020	0.00059	−0.00963	0.02795	0.00000	−0.05507	0.00315	−0.01768	0.00360	0.00000
	p_y	0.00000	0.00149	0.00267	−0.05091	0.00000	0.21893	−0.15007	−0.31841	−0.05979	0.00000
		0.00001	−0.00194	0.00163	−0.05030	0.00000	0.16367	−0.11042	−0.22758	−0.04473	0.00000
		0.00007	0.00046	−0.00338	0.02083	0.00000	0.03093	−0.04499	−0.12489	−0.01858	0.00000
		−0.00017	−0.00025	0.00878	−0.00024	0.00000	0.04445	−0.00625	−0.03107	−0.01938	0.00000
	p_z	0.00000	0.00000	0.00000	0.00000	0.00287	0.00000	0.00000	0.00000	0.00000	0.49589
		0.00000	0.00000	0.00000	0.00000	0.00151	0.00000	0.00000	0.00000	0.00000	0.36219
		0.00000	0.00000	0.00000	0.00000	0.00225	0.00000	0.00000	0.00000	0.00000	0.27064
		0.00000	0.00000	0.00000	0.00000	−0.00504	0.00000	0.00000	0.00000	0.00000	0.06441
	d_{xx}	0.00011	−0.00071	0.00459	−0.04828	0.00000	0.03487	0.00075	0.02388	0.00435	0.00000
	d_{xy}	0.00000	−0.00015	−0.00003	−0.00326	0.00000	0.01019	−0.00049	0.01345	0.00197	0.00000
	d_{xz}	0.00000	0.00000	0.00000	0.00000	0.00000	0.00000	0.00000	0.00000	0.00000	−0.01204
	d_{yy}	0.00013	−0.00087	0.00489	−0.05094	0.00000	−0.02947	0.02013	0.02721	0.00579	0.00000
	d_{yz}	0.00000	0.00000	0.00000	0.00000	−0.00008	0.00000	0.00000	0.00000	0.00000	−0.01603
	d_{zz}	0.00015	−0.00163	0.00506	−0.07041	0.00000	0.00163	0.00292	0.00176	0.00061	0.00000

Table 7 (continued)

Orbital number		1	2	3	4	5	6	7	8	9	10
Energy		−20.59077	−20.53238	−1.37911	−1.32183	−0.74492	−0.69553	−0.61539	−0.55121	−0.53633	−0.47945
Orbital Coefficients											
Center	Type										
H_1	s	−0.00021	−0.00004	−0.04771	−0.00353	0.06986	−0.01179	−0.03870	0.01013	0.00103	−0.00105
		−0.00203	0.00026	−0.14039	−0.00938	0.32830	−0.06041	−0.19099	0.05112	0.00753	−0.00571
		0.00142	−0.00090	−0.01258	−0.01219	−0.08628	0.01337	0.00507	−0.00619	−0.00322	−0.02562
	p_x	−0.00047	0.00000	−0.00903	0.00083	0.01808	0.00272	0.00918	−0.00227	0.00002	−0.00055
	p_y	0.00000	0.00000	0.00003	0.00009	−0.00016	0.00018	−0.00022	−0.00463	0.02886	0.00000
	p_z	0.00087	−0.00001	0.01432	0.00149	−0.00946	0.00621	0.01817	−0.00442	−0.00075	0.00030
H_2	s	−0.00021	−0.00004	−0.04771	−0.00353	−0.06986	−0.01179	−0.03870	0.01013	0.00103	0.00105
		−0.00203	0.00026	−0.14039	−0.00938	−0.32830	−0.06041	−0.19099	0.05112	0.00753	0.00571
		0.00142	−0.00090	−0.01258	−0.01219	0.08628	0.01337	0.00507	−0.00619	−0.00322	0.02562
	p_x	−0.00047	0.00000	−0.00903	0.00083	−0.01808	0.00272	0.00918	−0.00227	0.00002	0.00055
	p_y	0.00000	0.00000	0.00003	0.00009	0.00016	0.00018	−0.00022	−0.00463	0.02886	0.00000
	p_z	−0.00087	0.00001	−0.01432	−0.00149	−0.00946	−0.00621	−0.01817	0.00442	0.00075	0.00030
H_3	s	−0.00005	−0.00018	−0.00368	0.04725	0.00000	0.06792	−0.00853	0.04138	0.00648	0.00000
		0.00029	−0.00214	−0.02021	0.14067	0.00000	0.31598	−0.04647	0.21350	0.03189	0.00000
		0.00024	0.00493	−0.05871	0.11831	0.00000	−0.12588	−0.05998	0.07559	0.02973	0.00000
	p_x	−0.00002	−0.00101	−0.00135	0.01661	0.00000	0.01741	−0.01231	0.01422	0.00165	0.00000
	p_y	−0.00001	0.00012	0.00042	−0.00244	0.00000	0.00729	−0.00741	−0.02088	−0.00235	0.00000
	p_z	0.00000	0.00000	0.00000	0.00000	0.00104	0.00000	0.00000	0.00000	0.00000	0.02849
H_4	s	−0.00002	−0.00026	−0.00219	0.04758	0.00000	−0.06554	0.03008	0.03631	0.00754	0.00000
		0.00013	−0.00153	−0.01313	0.15404	0.00000	−0.31910	0.14615	0.20020	0.04166	0.00000
		−0.00038	0.00027	0.02039	−0.01606	0.00000	0.08192	0.01176	0.00077	−0.01410	0.00000
	p_x	−0.00001	0.00034	0.00082	−0.00705	0.00000	−0.00426	−0.00295	−0.02468	−0.00390	0.00000
	p_y	0.00001	−0.00081	−0.00165	0.01718	0.00000	−0.02013	0.00616	0.00407	0.00071	0.00000
	p_z	0.00000	0.00000	0.00000	0.00000	0.00023	0.00000	0.00000	0.00000	0.00000	0.03026

[a] Dimeric water in the linear perpendicular geometry; geometry parameters are defined in Fig. 2; $\psi = 52.26°$, $\varphi = 0°$, and $\vartheta = 0°$.

[b] Orbital energies in a.u.

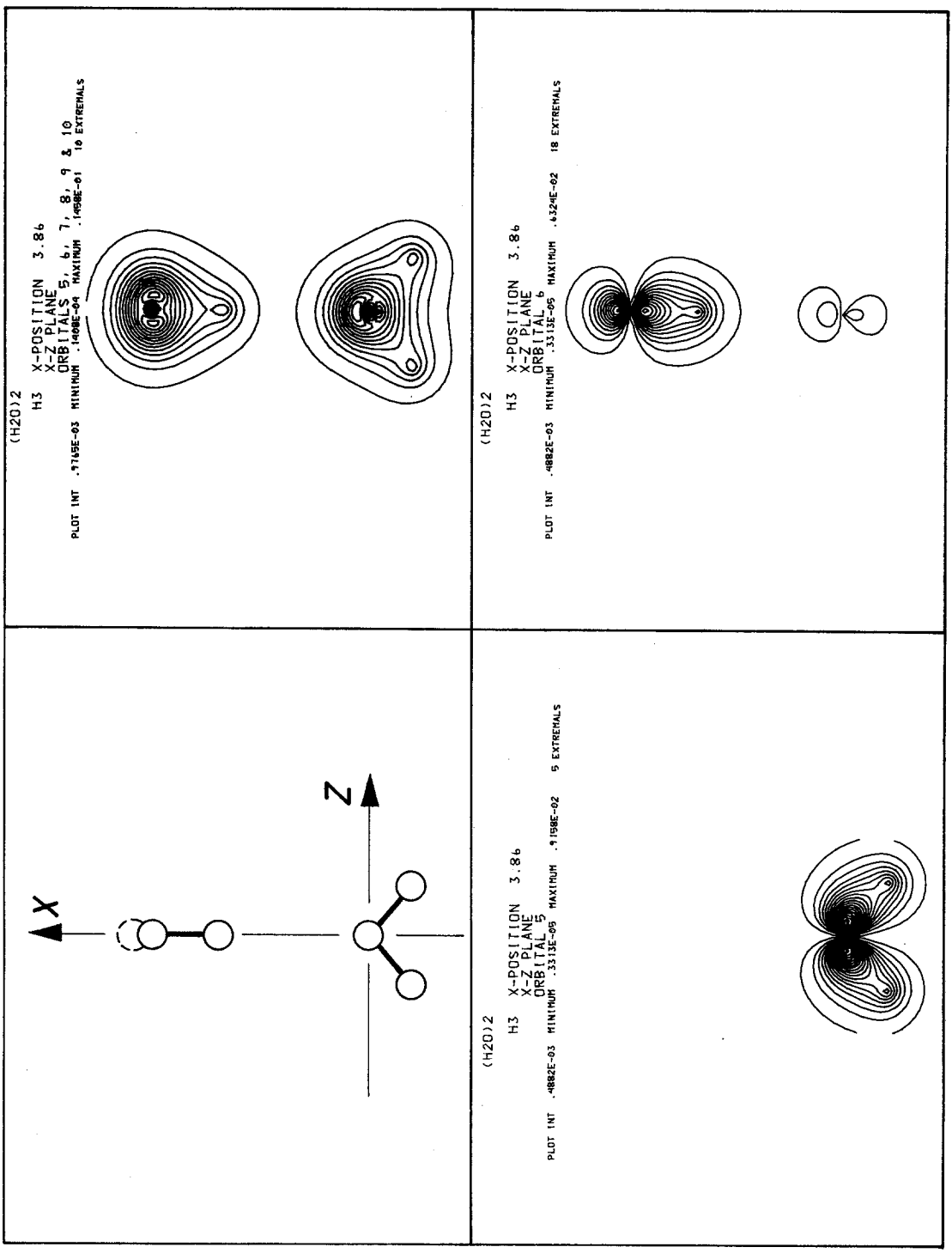

Fig. 5a and b. Charge density contour maps for dimeric water in the linear perpendicular geometry at an oxygen-oxygen separation of $d(O_1O_2) = 3.00$ Å: a) in the $x-z$ plane and b) in the $x-y$ plane

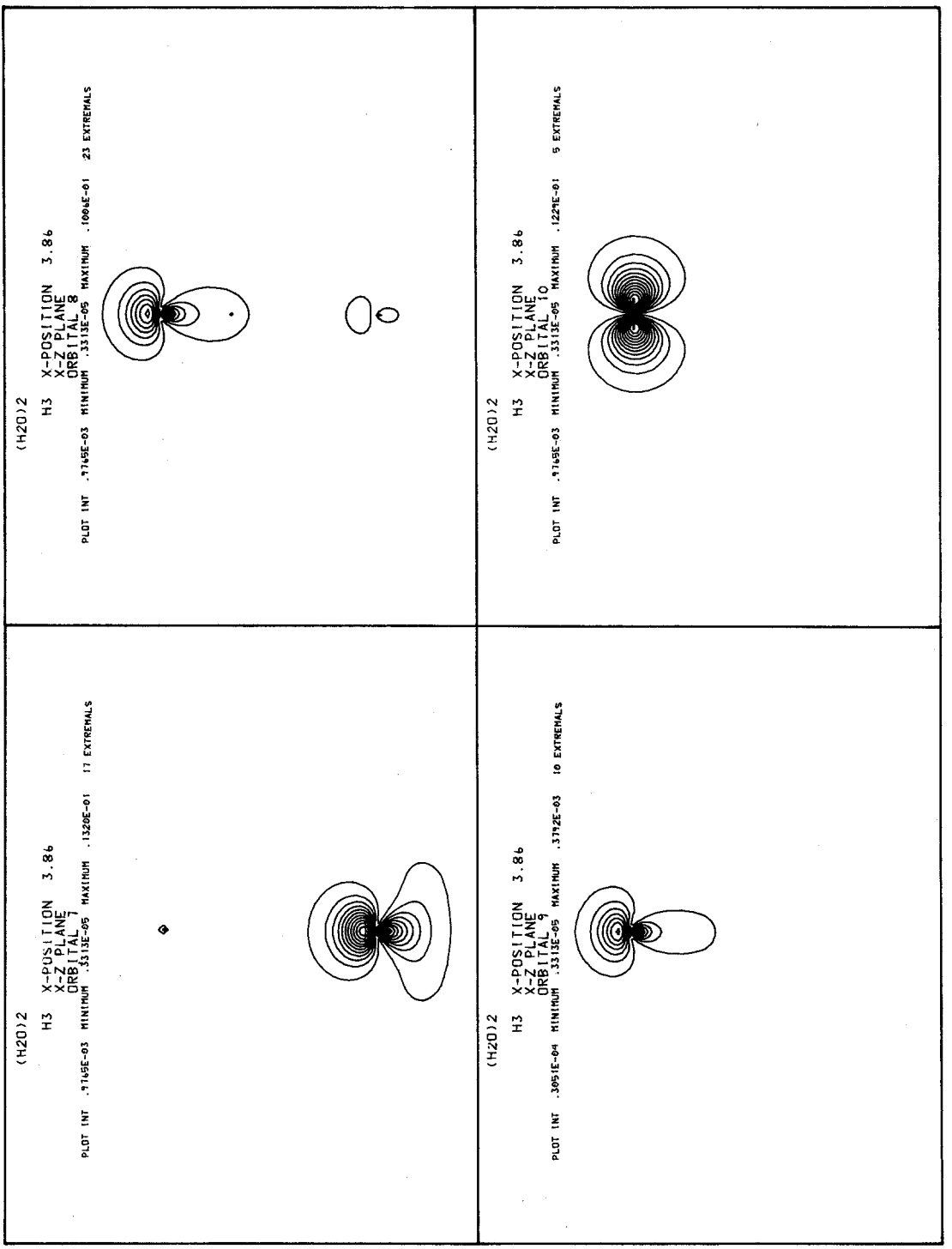
(H2O)2
H3 X-POSITION 3.86
X-Z PLANE
ORBITAL 8
PLOT INT .9765E-03 MINIMUM .3313E-05 MAXIMUM .1066E-01 23 EXTREMALS
(H2O)2
H3 X-POSITION 3.86
X-Z PLANE
ORBITAL 10
PLOT INT .9765E-03 MINIMUM .3313E-05 MAXIMUM .1229E-01 5 EXTREMALS
(H2O)2
H3 X-POSITION 3.86
X-Z PLANE
ORBITAL 7
PLOT INT .9765E-03 MINIMUM .3313E-05 MAXIMUM .1320E-01 17 EXTREMALS
(H2O)2
H3 X-POSITION 3.86
X-Z PLANE
ORBITAL 9
PLOT INT .3051E-04 MINIMUM .3313E-05 MAXIMUM .3792E-03 10 EXTREMALS

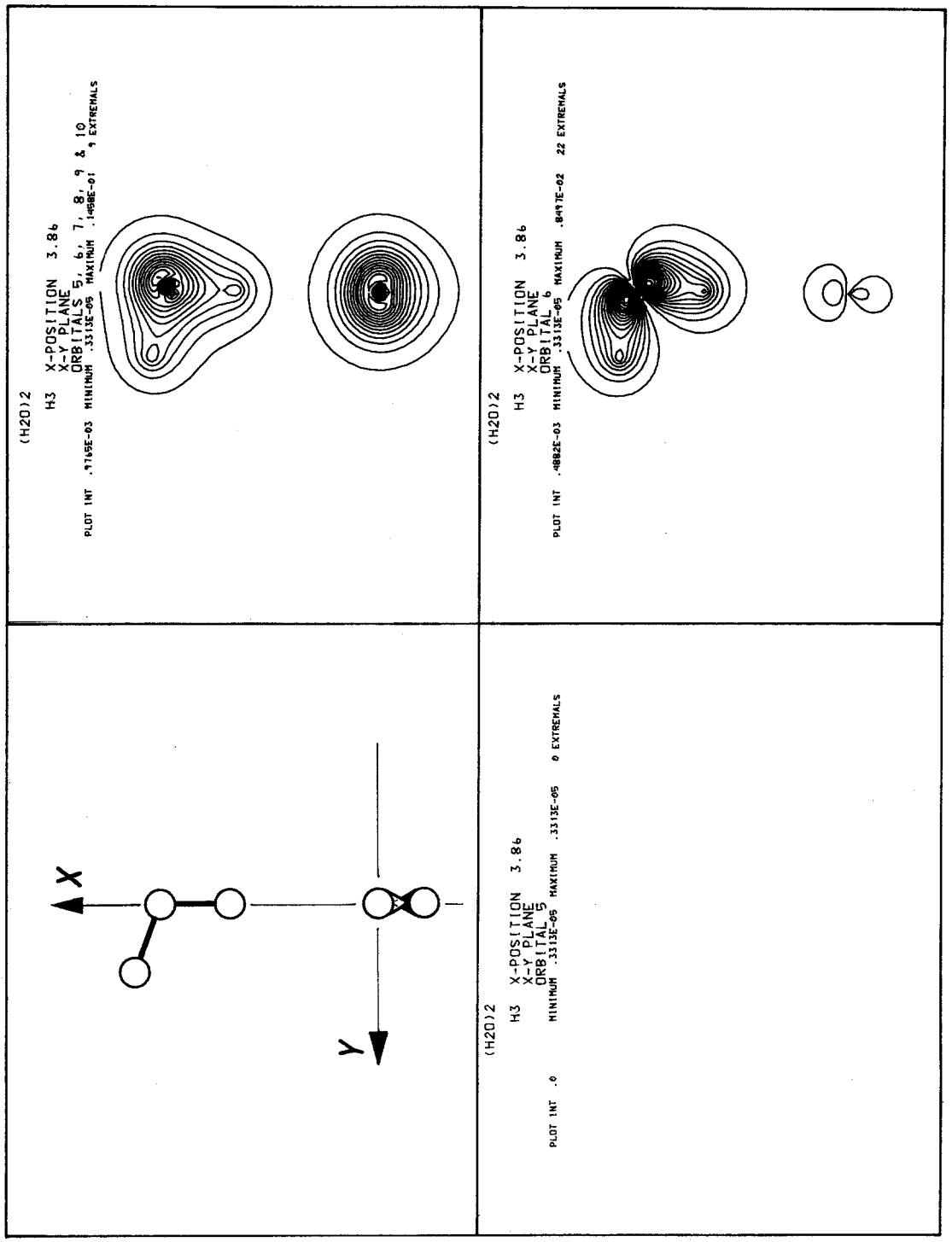
(H2O)2
H3 X-POSITION 3.86
X-Y PLANE
ORBITALS 5, 6, 7, 8, 9 & 10
PLOT INT .4715E-03 MINIMUM .3313E-05 MAXIMUM .1456E-01 9 EXTREMALS
(H2O)2
H3 X-POSITION 3.86
X-Y PLANE
ORBITAL 6
PLOT INT .4882E-03 MINIMUM .3313E-05 MAXIMUM .8497E-02 22 EXTREMALS
X
Y
(H2O)2
H3 X-POSITION 3.86
X-Y PLANE
ORBITAL 5
PLOT INT .0 MINIMUM .3313E-05 MAXIMUM .3313E-05 0 EXTREMALS

Fig. 5b

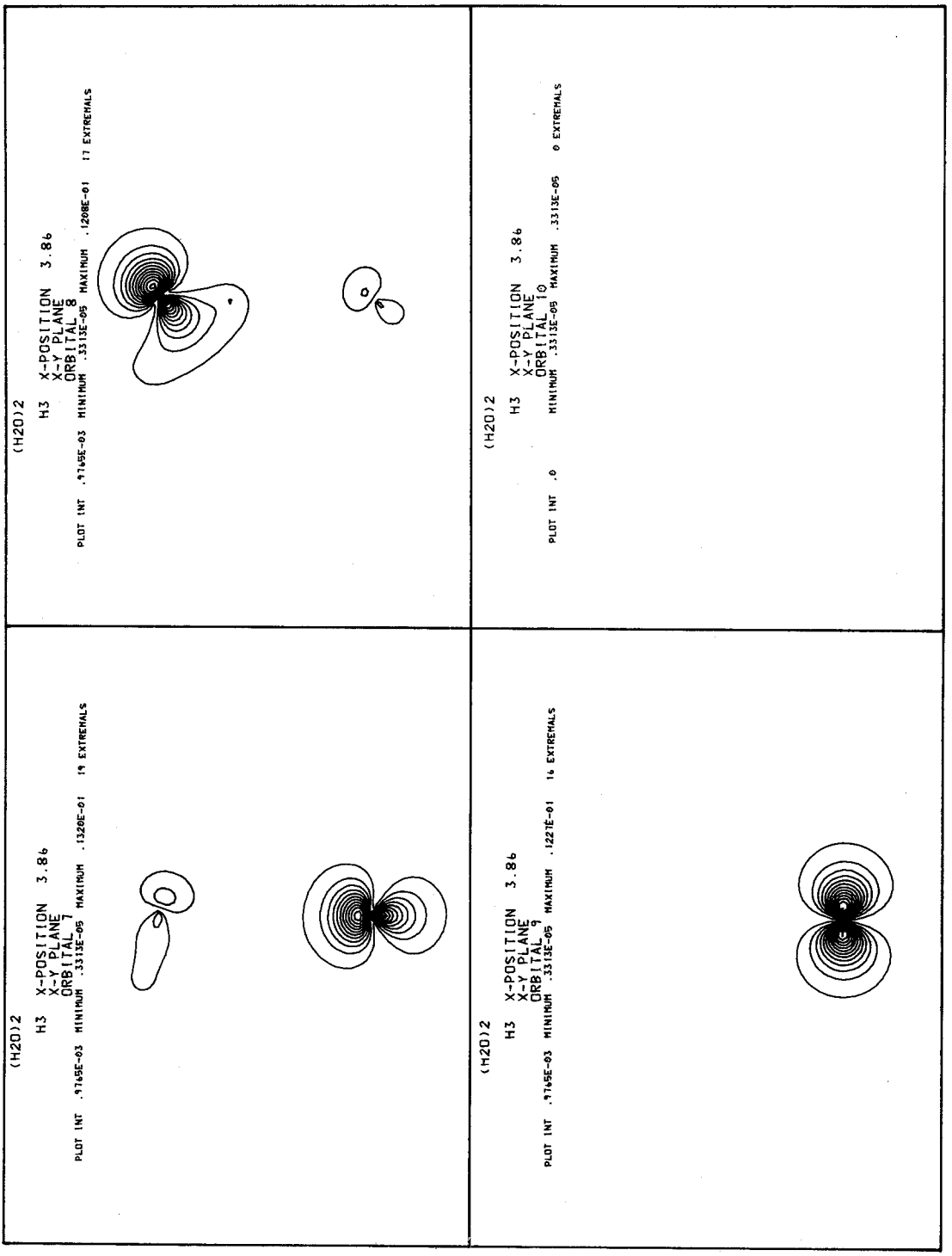
(H2O)2
H3 X-POSITION 3.86
X-Y PLANE
ORBITAL 8
PLOT INT .9765E-03 MINIMUM .3313E-05 MAXIMUM .1208E-01 17 EXTREMALS
(H2O)2
H3 X-POSITION 3.86
X-Y PLANE
ORBITAL 10
PLOT INT .0 MINIMUM .3313E-05 MAXIMUM .3313E-05 0 EXTREMALS
(H2O)2
H3 X-POSITION 3.86
X-Y PLANE
ORBITAL 7
PLOT INT .9765E-03 MINIMUM .3313E-05 MAXIMUM .1320E-01 19 EXTREMALS
(H2O)2
H3 X-POSITION 3.86
X-Y PLANE
ORBITAL 9
PLOT INT .9765E-03 MINIMUM .3313E-05 MAXIMUM .1227E-01 16 EXTREMALS

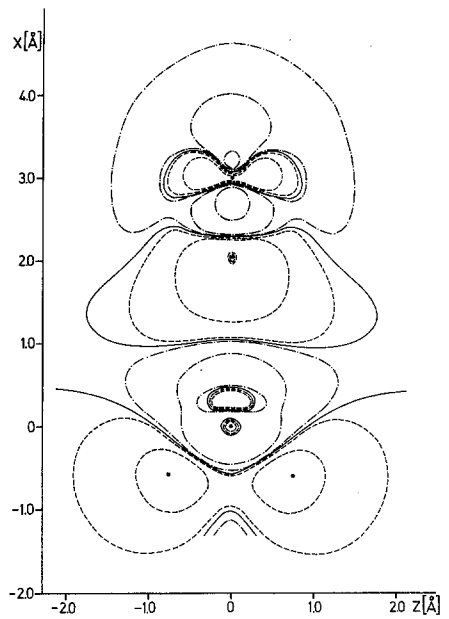

Fig. 6a

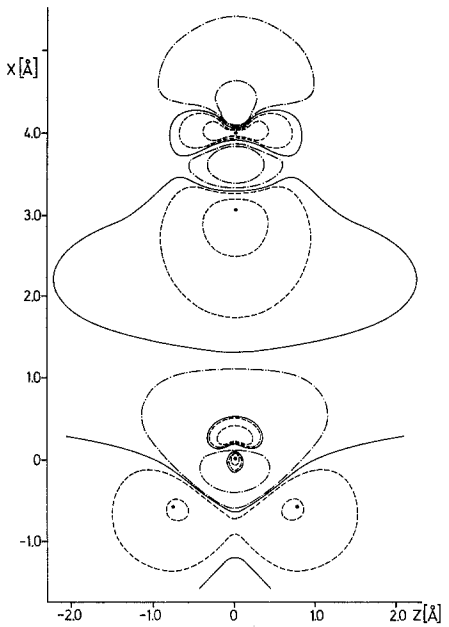

Fig. 6b

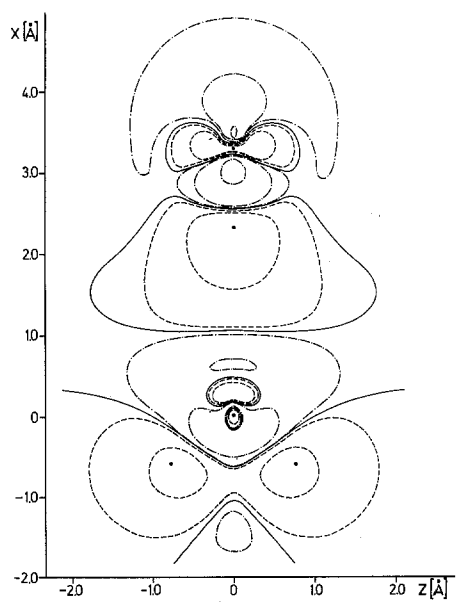

Fig. 6c

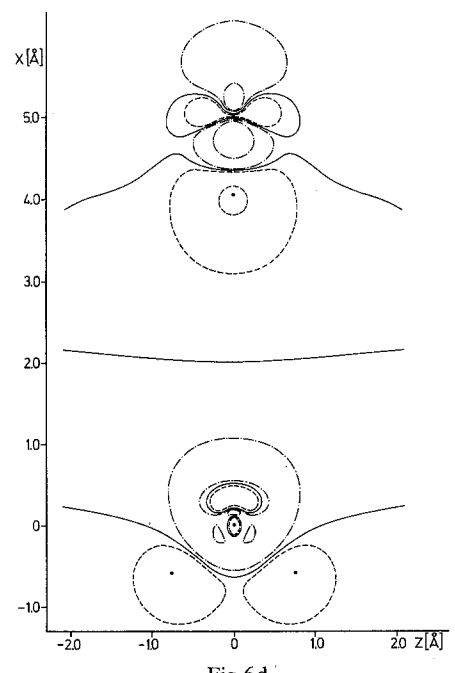

Fig. 6d

Fig. 6a – e. Charge density difference countour maps for dimeric water in the linear perpendicular geometry for different oxygen-oxygen distances in the $x-z$ plane: ——— Zero, —·—·—· positive, and — — — negative charge density difference contours, with relative heights: +1.0, +0.1, +0.01, +0.001, +0.0001, +0.0, −0.0001, −0.001, −0.01, −0.1, −1.0 at an oxygen-oxygen separation of: a) $d(O_1O_2) = 3.00$ Å; b) $d(O_1O_2) = 3.30$ Å; c) $d(O_1O_2) = 4.00$ Å; d) $d(O_1O_2) = 5.00$ Å; e) $d(O_1O_2) = 7.00$ Å

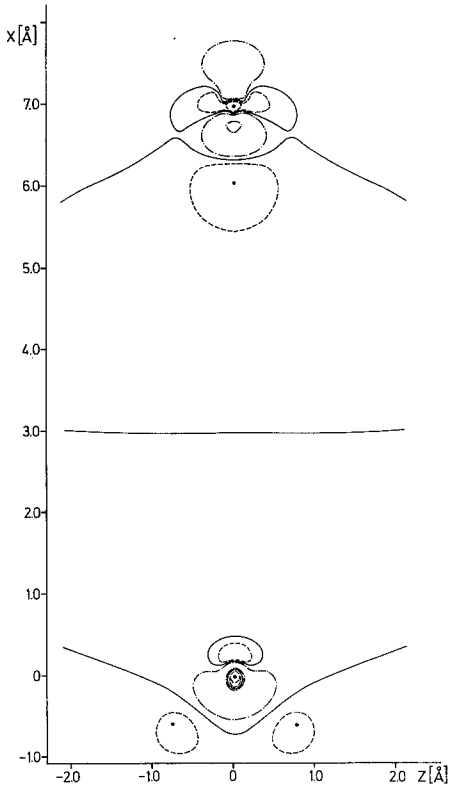

Fig. 6e

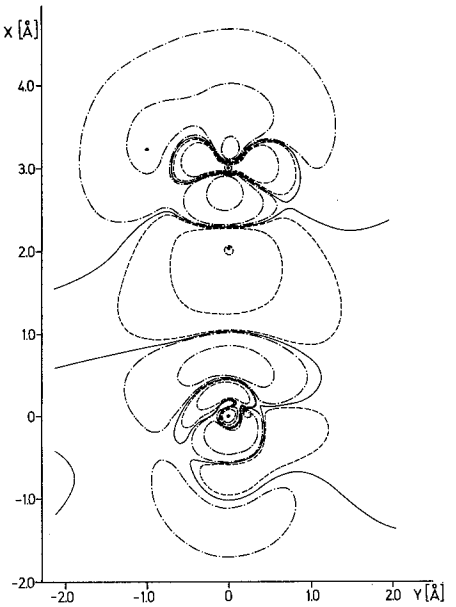

Fig. 7. Charge density difference contour maps for dimeric water in the linear perpendicular geometry at an oxygen-oxygen separation of $d(O_1O_2) = 3.00$ Å in the $x - y$ plane. For the explanation of the contour lines compare Fig. 6

Table 8. *Molecular orbital energies for dimeric water for different distances* $d(O_1O_2)$[a, b]

MO	$R(O_1O_2)$ 3.0	3.3	4.0	5.0	7.0	11.0
1	−20.59077	−20.58565	−20.57828	−20.57322	−20.56934	−20.56717
2	−20.53238	−20.54010	−20.54947	−20.55563	−20.56078	−20.56381
3	− 1.37911	− 1.37303	− 1.36539	− 1.36046	− 1.35663	− 1.35450
4	− 1.32183	− 1.32841	− 1.37705	− 1.34302	− 1.34809	− 1.35113
5	− 0.74492	− 0.73957	− 0.73239	− 0.72754	− 0.72376	− 0.72164
6	− 0.69553	− 0.69710	− 0.70409	− 0.71009	− 0.71521	− 0.71827
7	− 0.61539	− 0.60932	− 0.59887	− 0.59248	− 0.58809	− 0.58578
8	− 0.55121	− 0.55916	− 0.56870	− 0.57457	− 0.57945	− 0.58240
9	− 0.53633	− 0.53085	− 0.52313	− 0.51798	− 0.51405	− 0.51188
10	− 0.47945	− 0.48613	− 0.49472	− 0.50056	− 0.50552	− 0.50851

[a] Dimeric water in the linear perpendicular geometry; geometry parameters are defined in Fig. 2; $\psi = 52.26°$, $\varphi = 0°$, and $\vartheta = 0°$.

[b] Orbital energies in a.u., R in Å.

for the linear perpendicular structure for different oxygen-oxygen distances in the zx- and xy-planes, resp., and are displayed in Figs. 6 and 7. The charge difference has been taken between the electron densities computed for the two interacting water molecules and the two isolated water molecules as reference systems.

An analysis of the electron density difference maps (Figs. 6 and 7) shows the following characteristic features: the mutual interaction has changed the charge distribution at *all* nuclei, rather than only in the bond region itself. In the electron donor system the charge density has decreased at the hydrogens and increased at the oxygen nucleus with a slight polarization towards the hydrogen bond. In the proton donor system a charge decrease is found at the proton located in the hydrogen bridge, an increase at the second hydrogen atom and a fairly complicated charge shift around the oxygen atoms. This shows that by the mutual interaction of the two water molecules through a hydrogen bridge an additional dipole moment is induced in both water molecules. These dipole moments are directed in a way that any additional hydrogen bond on water molecules which are already taking part in other hydrogen bonds will increase these additional dipole moments. This can be expected to lead to an increase of the hydrogen bond energy per bond and to a decrease of the hydrogen bond length on the formation of polymers. For the same reasons (increase of the additional induced dipole moments) polymer rings should be more stable than chains if the ring formation is possible without too much hindrance (change of the valence angles). This is in agreement with experimental results. Especially it means that the hydrogen bond energy is not additive. Similar conclusions have been reached by other authors [21, 22, 24, 25] and by direct calculations on higher polymers of water.

This effect of charge redistribution on hydrogen bond formation rules out any attempt to generalize the quantitative results obtained for the dimer to higher polymers of water. Moreover it is clear, that those approximative methods cannot give a proper description of the hydrogen bond which are based on the assumption of the unmodified charge density or on a three center model A–H——B.

Dipole Moment

By an analysis of the dipole moment some additional information about the charge distribution in a molecular system may be obtained. Therefore the dipole moment has been computed for dimeric water in the linear perpendicular geometry for different oxygen-oxygen distances. The results for the x- and y-components are listed in Table 9, the z-component is zero. In addition, the dipole moments (x- and y-components) calculated for the isolated water molecules in the two different positions as occurring in the dimeric system are listed. They are denoted μ' for the molecule ($O_1H_1H_2$) and μ'' for ($O_2H_3H_4$).

Assuming no mutual interaction, the total dipole moment of a system of two water molecules can be computed by simple vector addition of the individual dipole moments of the two subsystems (water molecules). The values calculated this way are $\mu_x = -1.400$ a.u. and $\mu_y = -0.687$ a.u. As can be seen from Table 9, the total dipole moment of the dimeric system is converging nicely against these values for large intersystem separations (large $d(O_1O_2)$). For the minimum energy geometry ($d(O_1O_2) = 3.00$ Å), the dipole moment components are higher by about $\Delta\mu_x = -0.15$ a.u. and $\Delta\mu_y = -0.02$ a.u. compared to the values computed for the equivalent structure of two noninteracting subsystems (water molecules). This indicates an overall charge shift along the positive x-direction

Table 9. *Dipole moment μ relative to oxygen O_1 of dimeric water for different distances $d(O_1O_2)$*[a,b]

	$d(O_1O_2)$	Total	Nucl.	Electr.	Molecular orbital									
					1	2	3	4	5	6	7	8	9	10
μ_x	3.00	−1.549	53.123	− 54.671	0.0005	−11.3381	0.5795	−10.9094	0.7915	− 9.9620	−1.7955	−10.5367	0.2252	−11.2782
	3.30	−1.498	58.792	− 60.290	0.0005	−12.4720	0.6171	−12.0709	0.7972	−11.7434	−0.8979	−12.1726	0.0638	−12.4122
	4.00	−1.450	72.020	− 73.470	0.0006	−15.1176	0.6410	−14.7272	0.8044	−14.6198	−0.3359	−15.1494	0.0939	−15.0600
	5.00	−1.427	90.918	− 92.345	0.0006	−18.8973	0.6463	−18.5045	0.8086	−18.4066	−0.2239	−19.0239	0.0952	−18.8394
	7.00	−1.409	128.713	−130.122	0.0006	−26.4557	0.6483	−26.0612	0.8108	−25.9617	−0.2130	−26.5880	0.0957	−26.3979
μ'_x[c]	—	−0.868	−2.214	1.346	0.0006		0.6492		0.8120		−0.2117		0.0960	
μ''_x[c]	3.00	−0.531	55.337	− 55.868		−11.3379		−10.9412		−10.8416		−11.4681		−11.2798
μ_y	3.00	−0.666	−1.751	1.085	0.0000	0.0005	0.0041	0.5150	0.0008	0.5791	0.0864	− 0.1881	0.0112	0.0758
	3.30	−0.672	−1.751	1.079	0.0000	0.0004	0.0027	0.5156	0.0007	0.6257	0.0281	− 0.1726	0.0032	0.0758
	4.00	−0.678	−1.751	1.073	0.0000	0.0004	0.0013	0.5150	0.0004	0.6415	0.0036	− 0.1665	0.0010	0.0759
	5.00	−0.682	−1.751	1.069	0.0000	0.0004	0.0008	0.5143	0.0003	0.6423	0.0012	− 0.1667	0.0005	0.0759
	7.00	−0.685	−1.751	1.066	0.0000	0.0004	0.0003	0.5136	0.0001	0.6423	0.0005	− 0.1671	0.0002	0.0759
μ'_y[c]	—	0.000	0.000	0.000	0.0000		0.0000		0.0000		0.0000		0.0000	
μ''_y[c]	3.00	−0.687	−1.751	1.065		0.0004		0.5134		0.6422		− 0.1674		0.0759

[a] Dimeric water in the linear perpendicular geometry; geometry parameters are defined in Fig. 2; $\psi = 52.26°$, $\varphi = 0°$, and $\vartheta = 0°$.

[b] Values of q in a.u., 1 a.u. = 2.541539 Debyes; d in a.u.

[c] For comparison the dipole moments μ' and μ'' for the "isolated" systems (water) $(O_1H_1H_2)$ and $(O_2H_3H_4)$, resp., are given.

towards the proton donor molecule. But this should in no way be interpreted as a charge transfer from one water molecule to the other, because only small charge shifts within the individual subsystems can be responsible for dipole moment changes of this order.

The components of the orbital dipole moments have been calculated relative to the origin of the coordinate systems (position of O_1). For the linear perpendicular geometry with the distance $d(O_1O_2)=3.00$ Å (min. energy structure) the components of the orbital dipole moments μ may be compared against those of μ' and μ''. It is found that orbitals 6 through 9 are considerably polarized towards the hydrogen bond region. As was also indicated by inspection of the charge density contour lines these orbitals have already been identified as mainly taking part in the hydrogen bonding. The orbitals forming the OH-bond in the donor molecule and the lone-pair orbitals in both water molecules are most strongly polarized. Small polarization effects can even be noticed in the orbitals 3 and 4 (2*s*-orbitals on oxygen).

Hydrogen Bond Stretching and Infrared Spectra

The potential curve for the proton in the hydrogen bridge (H_3) has been calculated for the minimum energy structure over a wide range. The numerical results are listed in Table 5, lines 23 to 29. The equilibrium OH-bond length has been interpolated to be $d(H_3O_2)=0.9483$ Å. From this value and the equilibrium OH-bond length computed for water ($d(OH)=0.9443$ Å) the bond stretching has been computed to be 0.004 Å. This value is negligible small and well outside the numerical accuracy. For the proton (H_3) transfer from the proton donor water molecule to the proton acceptor molecule the potential energy increases permanently without passing an energy barrier. This process effectively "simulates" the reaction $H_2O+H_2O\rightarrow H_2OH^+ + OH^-$, and the result is an agreement with that of other authors [56].

The potential energy curves for the OH-stretching in water and in the proton donor molecule of dimeric water are mapped in Fig. 8. The minima of both curves have been chosen as common origin and the curves have been shifted accordingly. It is found that the energy curve is slightly softer for the OH-stretching in the dimer than in the monomer. This explains qualitatively the low frequence shift of the IR-spectra on hydrogen bond formation, assuming that the OH-stretching in the proton donor molecule of the dimer is the one most effected by this bonding. Quantitative quantummechanical calculations of IR-spectra for polyatomic molecules are presently still out of range.

A large IR intensity increase of the fundamental OH-stretching band by a factor of 12 on hydrogen bond formation has been observed experimentally [54]. The relative intensity of the dimer and monomer can be shown to be proportional to [22].

$$\frac{|\partial\mu/\partial(\Delta d(\mathrm{OH}))|^2 \text{ dimer}}{|\partial\mu/\partial(\Delta d(\mathrm{OH}))|^2 \text{ monomer}}\,.$$

The dipole moments μ for a number of OH-distances d(OH) in the monomer and in the proton donor molecule of the dimer are given in Table 10. As can

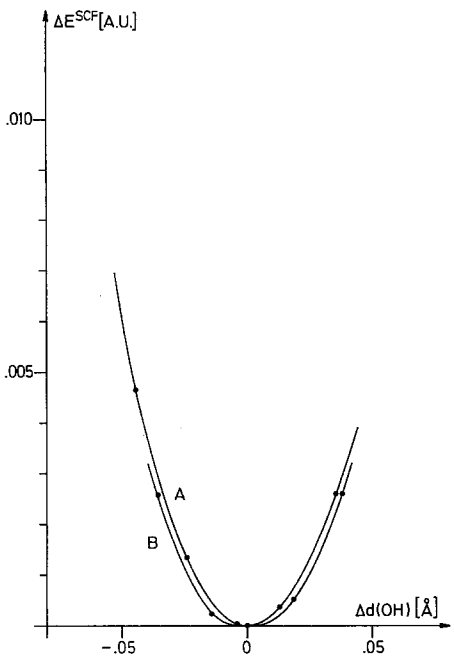

Fig. 8. Energy curve for the OH-stretching in water (*A*), and for the OH-stretching in the proton donor molecule of dimeric water (*B*)

Table 10. *Total* SCF-*energies and dipole moments for different* OH-*distances in water and dimeric water*[a]

d(OH)[b] Å	E^{SCF} a.u.	μ a.u.
H_2O-monomer		
0.8800	−76.042016	0.839434
0.9200	−76.051033	0.854655
0.9572	−76.051990	0.868342
0.9800	−76.049759	0.876260
1.0200	−76.041731	1.062675
H_2O-dimer		
0.9110	−152.10919	—
0.9310	−152.11152	1.664212
0.9572	−152.11167	1.685921
0.9640	−152.11126	—
0.9840	−152.10914	1.708707

[a] Water in the experimental geometry configuration; and dimeric water in the theoretical minimum energy geometry.

[b] Distances d(OH) in water, and in the proton donor molecule of dimeric water.

be seen from Fig. 9 there is a linear dependence of the dipole moment over a wide range of OH distances. From these results, an IR intensity increase by a factor of 5.3 has been calculated theoretically for the dimer. This is only about 50% of the experimental value. The discrepancy is most likely due to the fact that the experi-

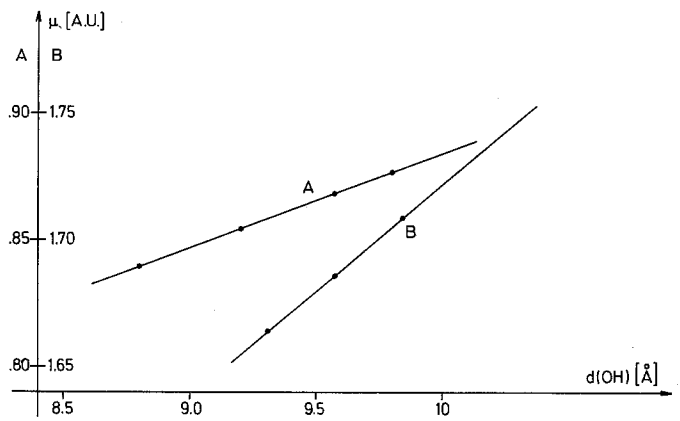

Fig. 9. Dipole moments as function of the OH-distances in water (*A*), and of the OH-distances of the proton donor molecule in dimeric water

mental results are not due to dimers only, but to a large extent to higher polymers to be expected in water.

Magnetic Shielding and Proton Magnetic Resonance Spectra

As indicated already, proton magnetic resonance signals are usually displaced to lower field by formation of a hydrogen bond [4, 42]. This shift arises, because the magnetic field experienced by the proton is modified when a hydrogen bond is formed. By definition a low field shift is related to a decrease of the total average magnetic shielding. The "proton shifts" (which really are shifts of chemical shifts) have been obtained for a number of substances by measuring the chemical shifts in the liquid and in the gas phase, and associating the difference, if any, to the formation of higher polymers in the liquid phase by hydrogen bonding. For water, a proton shift of $\sigma = -4.58$ ppm was found [43].

Very qualitatively the smaller average magnetic shielding on hydrogen bond formation can be explained by a decrease of the electron density near the proton. By inspection of the electron density difference maps (Figs. 6 and 7) it can be seen, that there really is a decrease in charge density around the proton in the hydrogen bond.

The total average magnetic shielding is the sum of a paramagnetic and a diamagnetic term. Both quantities can be calculated by rigorous quantum mechanical methods [45]. The diamagnetic shielding is only dependent on the groundstate wavefunction while the paramagnetic contribution depends on the excited states as well. Therefore the latter is rather hard to get this way and is more easily obtained from spin coupling constants [44]. The diamagnetic shielding is calculated from the electronic part of the potential (Table 11) to be $\sigma^d(\mathrm{H})_{(\mathrm{H_2O})_2} = 146.14$ ppm. This value is about 44.13 ppm higher than the result obtained for the monomer (Table 4). No data are available to compute the paramagnetic shielding in the dimer by one of the methods indicated. It is therefore impossible to calculate the total average magnetic shielding theoretically. The

Table 11. *Potential ϕ at oxygen and hydrogen in dimeric water*[a,b]

	$\phi(O_1)$	$\phi(H_1)$[c]	$\phi(O_2)$	$\phi(H_3)$	$\phi(H_4)$
Total	−22.3060	−0.9680	−22.3650	−1.0270	−1.0240
Nuclear	2.9330	6.2530	2.8060	7.2310	6.2920
Electronic	−25.2390	−7.2210	−25.1700	−8.2590	−7.3160
MO 1	−15.2806	−1.1058	− 0.3528	−0.5180	−0.3140
2	− 0.3528	−0.2888	−15.2806	−1.1058	−1.1058
3	− 0.2997	−1.2434	− 0.3412	−0.4831	−0.3030
4	− 0.3744	−0.3016	− 2.2946	−1.2431	−1.2515
5	− 0.7885	−1.3780	− 0.3258	−0.2588	−0.2933
6	− 0.5018	−0.3643	− 1.6555	−1.3265	−1.2789
7	− 1.7617	−0.9443	− 0.5921	−0.6206	−0.4876
8	− 0.4981	−0.3504	− 1.8687	−1.0193	−0.9777
9	− 2.0315	−0.9569	− 0.3916	−0.5106	−0.3208
10	− 0.3498	−0.2878	− 2.0645	−0.9729	−0.9735

[a] Dimeric water in the linear perpendicular geometry; geometry parameters are defined in Fig. 2; $\psi = 52.26°$, $\varphi = 0°$, $\vartheta = 0°$.

[b] In a.u., 1 a.u. = 9.07618 esu/cm.

[c] $\phi(H_2) = +\phi(H_1)$.

Table 12. *Average diamagnetic shielding σ^d_{AV} of dimeric water for different distances $d(O_1O_2)$*[a]

$d(O_1O_2)$ Å	$\sigma^d_{AV}(O_1)$	$\sigma^d_{AV}O_2)$	$\sigma^d_{AV}(H_1 = H_2)$	$\sigma^d_{AV}(H_3)$	$\sigma^d_{AV}(H_4)$
3.00	446.62169	445.40831	127.78462	146.14269	129.46589
3.30	443.63875	442.62608	125.87599	140.67435	127.28125
4.00	438.48181	437.79075	122.33391	132.00461	123.32809
5.00	433.67618	433.23796	118.75532	124.73653	119.42588
7.00	428.22021	427.99455	114.37396	117.31989	114.73966
∞	414.75264	414.75264	102.01591	102.01591	102.01591

[a] Dimeric water in the linear perpendicular geometry; geometry parameters are defined in Fig. 2; $\psi = 52.26°$, $\varphi = 0°$, and $\vartheta = 0°$.

total average magnetic shielding of the dimer of $\sigma_{AV}(H)_{(H_2O)_2} = 25.62$ ppm is obtained from the value of the monomer of $\sigma_{AV}(H)_{H_2O} = 30.20$ ppm [36] and the proton shift of $\sigma_{AV}(H) = -4.58$ ppm. From the total average magnetic shielding of the dimer and the diamagnetic term the paramagnetic shielding is calculated to be $\sigma^p(H)_{(H_2O)_2} = -120.52$ ppm. The absolute values of both the paramagnetic and the diamagnetic shielding thus increase for the dimer as predicted by the theoretical formula. They cancel largely.

The results for the diamagnetic shielding are given for all nuclei in dimeric water for different subsystem separations in Table 12.

Acknowledgement. This study was done while the author was visiting the IBM Research Laboratories, San Jose, California/USA. It is a pleasure to thank Prof. Dr. L. Biermann for making this visit possible, IBM Germany for a grant supporting the visit, and Dr. A. H. Eschenfelder and his staff for the great hospitality at the IBM Laboratories and for the computer time made available. My thanks are especially due to Dr. E. Clementi for initializing this visit, for his constant support, and for his interest in the work.

References

1. Latimer, W. M., Rodebush, W. H.: J. Amer. chem. Soc. **42**, 1419 (1920).
2. Watson, J. D., Crick, F. H. C.: Nature **171**, 737 (1953).
3. Deryagin, B. V., Talaev, M. V., Fedyakin, N. N.: Dokl. Akad. Nauk. SSSR **165**, 597 (1965); transl. Proc. Akad. Sci. USSR Phys. Chem. **165**, 807 (1965).
4. Pimentel, G. C., McClellan, A. D.: The hydrogen bond, San Francisco: W. A. Freeman and Co. 1960.
5. For a most recent review on the spectroscopical aspects, see: Murthy, A. S. N., Rao, C. N. R.: Appl. Spectroscopy Rev. **2**, 69 (1968).
6. Pauling, L.: Proc. nat. Acad. Sci. **14**, 359 (1928).
7. For most recent reviews on the theoretical aspects, see: Sokolov, N. D.: Ann. Chim. (Paris) **10**, 497 (1965); Bratoz, S.: Advances quant. Chem. **3**, 209 (1966).
8. Sokolov, N. D.: Dokladi **58**, 611 (1947).
9. Pimentel, G. C.: J. chem. Physics **19**, 446 (1951).
10. Ocvirk, A., Ažman, A., Hadži, D.: Theoret. chim. Acta (Berl.) **10**, 187 (1968).
11. Pullman, A., Berthod, H.: Theoret. chim. Acta (Berl.) **10**, 461 (1968).
12. Murthy, A. S. N., Rao, C. N. R.: Chem. Physics Letters **2**, 123 (1968).
13. Schuster, P., Funck, Th.: Chem. Physics Letters **2**, 587 (1968).
14. Murthy, A. S. N., Davis, R. E., Rao, C. N. R.: Theoret. chim. Acta (Berl.) **13**, 81 (1969).
15. Pedersen, L.: Chem. Physics Letters **4**, 280 (1969).
16. Kollman, P. A., Allen, L. C.: J. Amer. chem. Soc. **92**, 753 (1970).
17. Ažman, A., Koller, J., Hadži, D.: Chem. Physics Letters **5**, 157 (1970).
18. Clementi, E.: J. chem. Physics **34**, 1468 (1961).
19. — McLean, A. D.: J. chem. Physics **36**, 745 (1962); compare: McLean, A. D., Yoshimine, M.: IBM Journal of Research and Development, Suppl. 1967.
20. — J. chem. Physics **46**, 3851 (1967), **47**, 2323 (1967); Clementi, E., Gayles, J. N.: J. chem. Physics **47**, 3837 (1967).
21. Morokuma, K., Pedersen, L.: J. chem. Physics **48**, 3275 (1968).
22. Kollman, P. A., Allen, L. C.: J. chem. Physics **51**, 3286 (1969).
23. Diercksen, G. H. F.: Chem. Physics Letters **4**, 373 (1969).
24. Del Bene, J., Pople, J. A.: Chem. Physics Letters **4**, 426 (1969).
25. Hankins, D., Moskowitz, J. W., Stillinger, F. H.: Chem. Physics Letters **4**, 527 (1970).
26. Morokuma, K., Winick, J. R.: J. chem. Physics **52**, 1301 (1970).
27. Diercksen, G. H. F., Kraemer, W. P.: Chem. Physics Letters **5**, 570 (1970).
28. Kraemer, W. P., Diercksen, G. H. F.: Chem. Physics Letters **5**, 463 (1970).
29. Roothaan, C. C.: Rev. mod. Physics **23**, 69 (1951).
30. Veillard, A.: IBMOL/VERSION IV, Special IBM Technical Report, San José, California (1968).
31. Preuss, H., Diercksen, G.: Int. J. quant. Chemistry **1**, 605 (1967).
32. Neumann, D., Moskowitz, J. W.: J. chem. Physics **49**, 2056 (1968).
33. Kortzeborn, R. N.: Special IBM Technical Report, San José, California (1969).
34. Salez, C., Veillard, A.: Theoret. chim. Acta (Berl.) **11**, 441 (1968).
35. For the notation see: Moskowitz, J. W., Harrison, M. C.: J. chem. Physics **43**, 3550 (1965).
36. Neumann, D., Moskowitz, J. W.: J. chem. Physics **48**, 2056 (1968).
37. Nelson, R. D., Lide, D. R., Maryott, A. A.: Selected Values of Electric Dipole Moments for Molecules in the Gas Phase, National Standard Reference Data Series – National Bureau of Standards 10 (1967).
38. Eisenberg, D., Pochan, J. M., Flygare, W. H.: J. chem. Physics **43**, 4531 (1965).
39. For a most recent review see [36].
40. Hamilton, W. C., Ibers, J. A.: Hydrogen bonding in solids, New York: W. A. Benjamin Inc. 1968.
41. Koopmans, T.: Physica **1**, 104 (1933).
42. Pople, J. A., Schneider, W. G., Bernstein, H. J.: High-resolution nuclear magnetic resonance, New York: McGraw-Hill 1959.
43. Schneider, W. G., Bernstein, H. J., Pople, J. A.: J. chem. Physics **28**, 601 (1958).
44. See for example: Flygare, W. H.: J. chem. Physics **41**, 793 (1964).
45. Ramsey, N. F.: Physic. Rev. **78**, 699 (1950).
46. de Paz, M., Ehrenson, S., Friedman, L.: J. chem. Physics **52**, 3362 (1970).
47. del Bene, J., Pople, J. A.: J. chem. Physics **52**, 4858 (1970).
48. Kollman, P. A., Allen, L. C.: J. chem. Physics **52**, 5085 (1970).

49. Allen, L.C., Kollman, P.A.: Submitted to J. Amer. chem. Soc.
50. Kollman, P.A., Allen, L.C.: Submitted to J. Amer. chem. Soc.
51. — — Submitted to J. Amer. chem. Soc.
52. Diercksen, G.H.F., Kraemer, W.P.: Chem. Physics Letters **6**, 419 (1970).
53. Kraemer, W.P., Diercksen, G.H.F.: Submitted to Chem. Physics Letters.
54. van Thiel, M., Becker, E.D., Pimentel, G.C.: J. chem. Physics **27**, 486 (1957).
55. Sabin, J.R., Harris, R.E., Archibald, T.W., Kollman, P.A., Allen, L.C.: Theoret. chim. Acta (Berl.) **18**, 235 (1970).
56. Fang, Y., De La Vega, J.R.: Chem. Physics Letters **6**, 117 (1970).
57. Diercksen, G.H.F., Kraemer, W.P.: Chem. Physics Letters, to be published.
58. Clementi, E., Mekl, J., v. Niessen, W.: J. chem. Physics, accepted for publication.

Geerd Diercksen
Max-Planck-Institut für
Physik und Astrophysik
BRD-8000, München, Föhringer Ring 6
Germany